

AD-A152 286

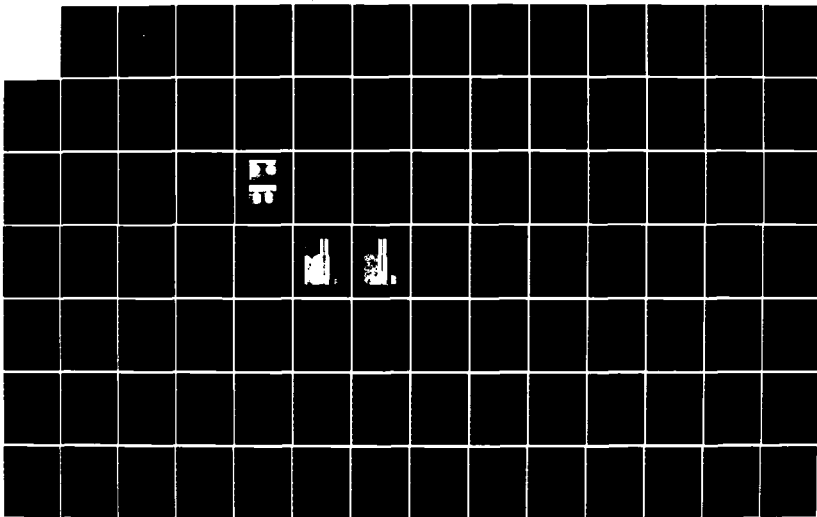
NUCLEATE POOL BOILING CHARACTERISTICS OF GEMA-T FINNED
SURFACES IN FREON-113(U) NAVAL POSTGRADUATE SCHOOL
MONTEREY CA R J PULIDO SEP 84

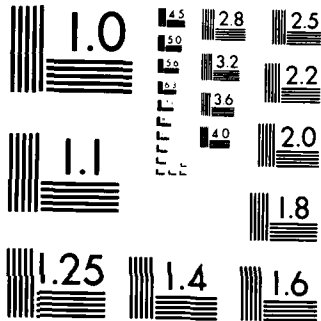
1/2

UNCLASSIFIED

F/G 29/13

NL





MICROCOPY RESOLUTION TEST CHART
NATIONAL BUREAU OF STANDARDS-1963-A

AD-A152 286

②

NAVAL POSTGRADUATE SCHOOL Monterey, California



DTIC
ELECTE
APR 11 1985
S B

THESIS

NUCLEATE POOL BOILING CHARACTERISTICS
OF GEWA-T FINNED SURFACES IN FREON-113

by

Ricardo J. Pulido ©.

September 1984

Thesis Advisor:

P. J. Marto

Approved for public release; distribution unlimited.

DTIC FILE COPY

85 08 20

UNCLASSIFIED

SECURITY CLASSIFICATION OF THIS PAGE (When Data Entered)

REPORT DOCUMENTATION PAGE		READ INSTRUCTIONS BEFORE COMPLETING FORM
1. REPORT NUMBER	2. GOVT ACCESSION NO. 41- A152286	3. RECIPIENT'S CATALOG NUMBER
4. TITLE (and Subtitle) Nucleate Pool Boiling Characteristics of Gewa-T Finned Surfaces in Freon-113		5. TYPE OF REPORT & PERIOD COVERED Master's Thesis; September 1984
		6. PERFORMING ORG. REPORT NUMBER
7. AUTHOR(s) Ricardo J. Pulido O.		8. CONTRACT OR GRANT NUMBER(s)
9. PERFORMING ORGANIZATION NAME AND ADDRESS Naval Postgraduate School Monterey, California 93943		10. PROGRAM ELEMENT, PROJECT, TASK AREA & WORK UNIT NUMBERS
11. CONTROLLING OFFICE NAME AND ADDRESS Naval Postgraduate School Monterey, California 93943		12. REPORT DATE September 1984
		13. NUMBER OF PAGES 100
14. MONITORING AGENCY NAME & ADDRESS (if different from Controlling Office)		15. SECURITY CLASS (of this report) Unclassified
		15a. DECLASSIFICATION/DOWNGRADING SCHEDULE
16. DISTRIBUTION STATEMENT (of this Report) Approved for public release; distribution unlimited.		
17. DISTRIBUTION STATEMENT of the abstract entered in Block 20, if different from Report)		
18. SUPPLEMENTARY NOTES		
19. KEY WORDS (Continue on reverse side if necessary and identify by block number) Nucleate Pool Boiling, Gewa-T Finned Surfaces.		
20. ABSTRACT (Continue on reverse side if necessary and identify by block number) Pool boiling heat-transfer measurements were made using seven Gewa-T copper tubes in R-113. The first tube (18-mm OD x 0.75 fins/mm x 0.25 mm gap) was tested under three conditions: (a) plain, (b) with four shrouds and (c) with up to 5 wires (0.13 mm diameter) wrapped in the inter-fin trough area. Verifying prior data, the shroud with longitudinal openings of 60° at the top and 8.5° at the bottom gave the best performance among the four		

DD FORM 1473
1 JAN 73

EDITION OF 1 NOV 65 IS OBSOLETE

S N O 02-15-014-5601

1 UNCLASSIFIED
SECURITY CLASSIFICATION OF THIS PAGE (When Data Entered)

UNCLASSIFIED

SECURITY CLASSIFICATION OF THIS PAGE (When Data Entered)

#20 - ABSTRACT - (CONTINUED)

shrouds tested. This shroud increased the boiling heat-transfer coefficient by 253 percent (over the smooth tube case) at a heat flux of $10,000 \text{ W/m}^2$, while it showed only a 18 percent increase at $100,000 \text{ W/m}^2$. When wire wraps were provided, in all cases, the heat-transfer coefficient was improved at all heat fluxes. The use of three wires gave the best performance with 341-percent increase in heat-transfer coefficient at $10,000 \text{ W/m}^2$ and a 130 percent increase at $100,000 \text{ W/m}^2$.

The next three Fewa-T tubes had dimensions of 25 mm OD \times 0.75 fins/mm with fin-tip gaps of 0.15, 0.25 and 0.35 mm, respectively. The last three Gewa-T tubes had the same dimensions except that the fin density was 1.02 fins/mm. For each of these fin densities, the 0.25 mm fin-tip gap produced the best boiling performance at all heat fluxes. Also, for a given fin-tip gap, the boiling performance increased with increase in fin density. For a fin-tip gap of 0.25 mm, the lower fin-density tube produced an 80-percent increase, while the higher fin density tube produced a 103-percent increase in the boiling heat-transfer coefficient.

Approved for public release; distribution unlimited.

Nucleate Pool Boiling Characteristics
of Gewa-T Finned Surfaces in Freon-113

by

Ricardo J. Pulido ©.
Lieutenant, Colombian Navy
B.S., Escuela Naval Almirante Padilla, 1979

Submitted in partial fulfillment of the
requirements for the degree of

MASTER OF SCIENCE IN MECHANICAL ENGINEERING

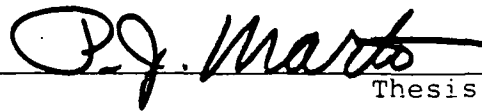
from the

NAVAL POSTGRADUATE SCHOOL
September 1984

Author



Approved by:



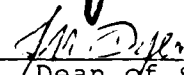
Thesis Advisor



Second Reader



Chairman, Department of Mechanical Engineering



Dean of Science and Engineering

ABSTRACT

Pool boiling heat-transfer measurements were made using seven Gewa-T copper tubes in R-113. The first tube (19-mm OD \times 0.75 fins/mm \times 0.25 mm gap) was tested under three conditions: (a) plain, (b) with four shrouds and (c) with up to 5 wires (0.13 mm diameter) wrapped in the inter-fin trough area. Verifying prior data, the shroud with longitudinal openings of 60° at the top and 8.5° at the bottom gave the best performance among the four shrouds tested. This shroud increased the boiling heat-transfer coefficient by 253 percent (over the smooth-tube case) at a heat flux of 10,000 W/m² while it showed only a 18 percent increase at 100,000 W/m². When wire wraps were provided, in all cases, the heat-transfer coefficient was improved at all heat fluxes. The use of three wires gave the best performance with 341-percent increase in heat-transfer coefficient at 10,000 W/m² and a 130 percent increase at 100,000 W/m².

The next three Gewa-T tubes had dimensions of 25 mm OD \times 0.75 fins/mm with fin-tip gaps of 0.15, 0.25 and 0.35 mm, respectively. The last three Gewa-T tubes had the same dimensions except that the fin density was 1.02 fins/mm. For each of these fin densities, the 0.25 mm fin-tip gap produced the best boiling performance at all heat fluxes. Also, for a given fin-tip gap, the boiling performance

increased with increase in fin density. For a fin-tip gap of 0.25 mm, the lower fin-density tube produced an 80-percent increase, while the higher fin density tube produced a 103-percent increase in the boiling heat-transfer coefficient.

Inspection For	
MI	<input checked="" type="checkbox"/>
MI	<input type="checkbox"/>
MI	<input type="checkbox"/>
Distribution/	
Availability Codes	
Dist	Avail and/or Special
A-1	



TABLE OF CONTENTS

I.	INTRODUCTION -----	13
	A. BACKGROUND -----	13
	B. THESIS OBJECTIVES -----	17
II.	EXPERIMENTAL APPARATUS -----	19
	A. REQUIREMENTS GOVERNING DESIGN -----	19
	B. TEST APPARATUS -----	19
	C. INSTRUMENTATION -----	24
	D. CALIBRATION OF THERMOCOUPLES -----	24
III.	EXPERIMENTAL PROCEDURES -----	28
	A. NORMAL OPERATION -----	28
	B. GEWA-T SURFACES -----	29
	C. HEAT-FLUX CALCULATION -----	31
IV.	RESULTS AND DISCUSSION -----	40
	A. DESIGNATION OF DATA FILES -----	40
	B. CIRCUMFERENTIAL UNIFORMITY OF HEAT FLUX AROUND HEATER ELEMENT -----	41
	C. LONGITUDINAL UNIFORMITY OF HEAT FLUX ALONG THE TEST SECTION -----	42
	D. PLOT ANALYSIS FOR PLAIN SURFACE -----	42
	E. REPEATABILITY WITH PREVIOUS DATA -----	48
	F. REPEATABILITY STUDY OF PRESENT WORK -----	48
	G. BOILING PERFORMANCE OF SMOOTH TUBE -----	51
	H. BOILING PERFORMANCE OF GEWA-T TUBES WITH SHROUDS -----	53
	I. PERFORMANCE OF GEWA-T TUBE WITH WIRE WRAPS IN INTER-FIN GAP -----	60

J.	BOILING PERFORMANCE OF TUBE 1 WITH 60° × 8.5° SHROUD AND THREE WIRES -----	65
K.	EFFECTS OF FIN-TIP GAP AND FIN DENSITY OF GEWA-T TUBES ON BOILING PERFORMANCE -----	65
V.	CONCLUSIONS -----	78
VI.	RECOMMENDATIONS -----	80
	APPENDIX A: COMPUTER PROGRAM -----	81
	APPENDIX B: SAMPLE CALCULATIONS -----	91
	A. TEST-SECTION DIMENSIONS -----	91
	B. MEASURED PARAMETERS -----	91
	C. PROPERTIES OF FREON-113 AT SATURATION TEMPERATURE -----	92
	D. HEAT-FLUX CALCULATION -----	92
	APPENDIX C: UNCERTAINTY ANALYSIS -----	96
	A. UNCERTAINTY IN SOURCE HEAT-TRANSFER RATE ----	96
	B. UNCERTAINTY IN SURFACE AREA -----	97
	C. UNCERTAINTY IN ΔT -----	97
	D. UNCERTAINTY IN HEAT FLUX -----	97
	E. UNCERTAINTY IN BOILING HEAT-TRANSFER COEFFICIENT -----	98
	LIST OF REFERENCES -----	99
	INITIAL DISTRIBUTION LIST -----	100

LIST OF FIGURES

1. Schematic of Test Apparatus -----	21
2. Thermocouple Radial and Angular Positions -----	22
3. Cross-Sectional View of Test Section -----	23
4. Thermocouple Calibration Curve -----	26
5. Optical Micrograph of Gewa-T Fin Profile, 50X -----	30
6. Geometry of Unenhanced Ends -----	33
7. Typical Nucleate Pool-Boiling Curve for a Gew-T Surface -----	43
8. Photograph of Gewa-T Surface at High Heat Flux ----	45
9. Photograph of Gewa-T Surface at Low Heat Flux ----	46
10. Reproducibility Test: Hernandez Run No. 3 Versus Present Work (GTLH05) -----	49
11. Reproducibility Test: Plain Gewa-T Tube 1 -----	50
12. Extrapolation to Smooth Tube (23.1 mm OD) from Smooth-Tube Data of Hernandez (19.61 mm OD) -----	52
13. Effect of 60° x 60° Shroud on Boiling Performance of Plain Gewa-T Tube 1 -----	55
14. Effect of 60° x 30° Shroud on Boiling Performance of Plain Gewa-T Tube 1 -----	56
15. Effect of 30° x 30° Shroud on Boiling Performance of Plain Gewa-T Tube 1 -----	57
16. Effect of 60° x 8.5° Shroud on Plain Gewa-T Tube 1 -----	58
17. Effect of Two Wires Wrapped in the Inter-fin Cavity of Tube 1 on Boiling Performance -----	61
18. Effect of Three Wires Wrapped in the Inter-fin Cavity of Tube 1 on Boiling Performance -----	62
19. Effect of Four Wires Wrapped in the Inter-fin Cavity of Tube 1 on Boiling Performance -----	63

20.	Effect of Five Wires Wrapped in the Inter-fin Cavity of Tube 1 on Boiling Performance -----	64
21.	Effect of Three Wires Wrapped in the Inter-fin Cavity with 60° x 8.5° Shroud on Gewa-T Tube 1 on Boiling Performance -----	66
22.	Boiling Performance of Gewa-T Tube 2 -----	68
23.	Boiling Performance of Gewa-T Tube 3 -----	69
24.	Boiling Performance of Gewa-T Tube 4 -----	70
25.	Boiling Performance of Gewa-T Tube 5 -----	71
26.	Boiling Performance of Gewa-T Tube 6 -----	72
27.	Boiling Performance of Gewa-T Tube 7 -----	73
28.	Enhancement Ratios of Gewa-T Tubes over Smooth Tubes Based on Nominal Area -----	75
29.	Enhancement Ratios of Gewa-T Tubes over Smooth Tube Based on Actual Area -----	77

NOMENCLATURE

$(T_W - T_{SAT})$	average wall superheat (K)
T_B	temperature at the base of the fins ($^{\circ}C$)
T_{SAT}	fluid saturation temperature ($^{\circ}C$)
T_{AVG}	average wall temperature ($^{\circ}C$)
Q_H	heat-transfer rate from the cartridge heater (W)
Q_F	heat-transfer rate through unenhanced end (W)
Q_{LOSS}	total heat-loss rate (W)
q	heat flux from the Gewa-T surface (W/m^2)
\bar{h}	average heat-transfer coefficient ($W/m^2.K$)
k_C	thermal conductivity of the copper (W/m.K)
k	thermal conductivity of Freon-113 liquid (W/m.K)
β	volumetric thermal expansion coefficient (1/K)
ν	kinematic viscosity (m^2/s)
α	thermal diffusivity (m^2/s)
ρ	density of Freon-113 (kg/m^3)
Nu	Nussel number
Ra	Rayleigh number
Pr	Prandtl number
V	voltage across the cartridge heater element (volts)
V_{RES}	voltage drop across the precision resistor (volts)
I	current through the heater element (amps)

R	resistance of the precision resistor (ohms)
O.D.	outside diameter of the Gewa-T tube (m)
D_1	diameter at the position of the thermocouples (m)
D_2	diameter at the base of the fins (m)
D_o	outside diameter of the unenhanced ends (m)
D_i	inside diameter of the unenhanced ends (m)
P	outside wall perimeter of the unenhanced ends (m)
H_F	fin height (m)
L	length of enhanced test section (m)
L_U	length of unenhanced ends (m)
L_C	corrected length of unenhanced ends (m)
t	tube thickness of unenhanced ends (m)
A_B	surface area at the base of the fins (m^2)
A_C	cross-sectional area of tube wall at the unenhanced ends (m^2)
A_S	outside surface area of the unenhanced ends (m^2)
g	gravitational acceleration (m/s^2)

excluded), and the two thermocouples for vapor and liquid temperature measurements were calibrated in an insulated, stainless-steel bath. The tubes were completely immersed into the bath, which was provided with a motor-driven mixer. The bath temperature was measured using a platinum-resistance thermometer accurate to ± 0.01 K.

Since the temperature measurements during this investigation ranged from 45°C to 60°C , thermocouple calibration was performed in the range of 45°C to 70°C . To begin the calibration process, hot water (at about 75°C) was added to the insulated container. Following proper mixing, all thermocouple readings were automatically recorded through the data-acquisition system. The bath temperature was measured using the platinum-resistance thermometer. To obtain other lower temperatures, small quantities of water were added to the bath, allowing 5 minutes for temperature stabilization of the test section.

The discrepancy (i.e., the platinum-resistance thermometer reading minus the thermocouple reading) was plotted against the thermocouple reading as shown in Figure 4. The second order polynomial curve shown in this figure was generated using the data from all seventeen thermocouples. However, for clarity, only three thermocouples were selected for data points from each tube. It is evident that the thermocouples in both tubes show similar discrepancies, the thermocouple readings have only about ± 0.1 K discrepancy around the

Plexiglas lid, which had been fitted with a rubber O-ring. Several holes were drilled in the lid to fix in place the test section extension, vent tube, connections for primary and secondary condensers, and two more thermocouples to sense both the bulk liquid and vapor temperatures. The Pyrex glass vessel with the attached fittings was placed on the plate heater, which served to maintain the liquid at saturation temperature. A secondary condenser was mounted external to the vessel.

C. INSTRUMENTATION

The power supply was connected to the cartridge heater through a voltage regulator and then to a Variac scaled from 0 to 120 VAC. This arrangement allowed fine adjustment for a stable feed voltage during the runs. A precision resistor of 2.031 ohms was connected in series with the cartridge heater to provide a measure of the current flow by reading the voltage drop across this element. A digital voltmeter was used to measure both the voltage across the resistor and the voltage across the cartridge heater. All the thermocouples were connected to a computer data acquisition system, and ambient conditions and voltage readings were supplied manually. The microcomputer processed all this information through a program included in Appendix A.

D. CALIBRATION OF THERMOCOUPLES

A total of fifteen wall thermocouples in tubes 1 and 7 (one thermocouple in tube 1 was defective, hence it was

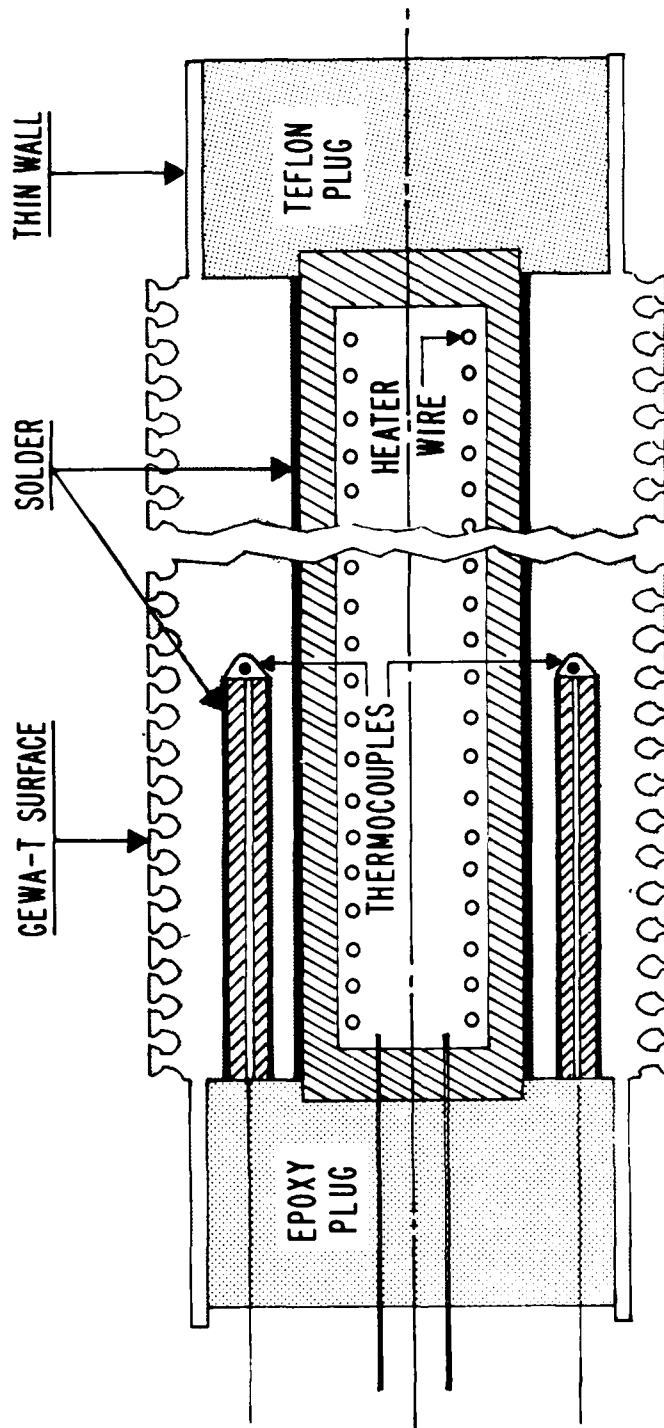


Figure 3. Cross-Sectional View of Test Section

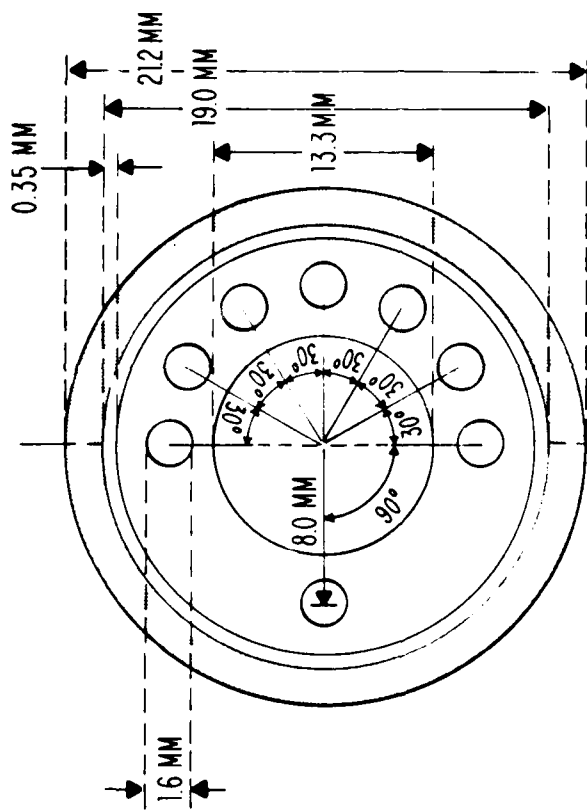


Figure 2. Thermocouple Radial and Angular Positions

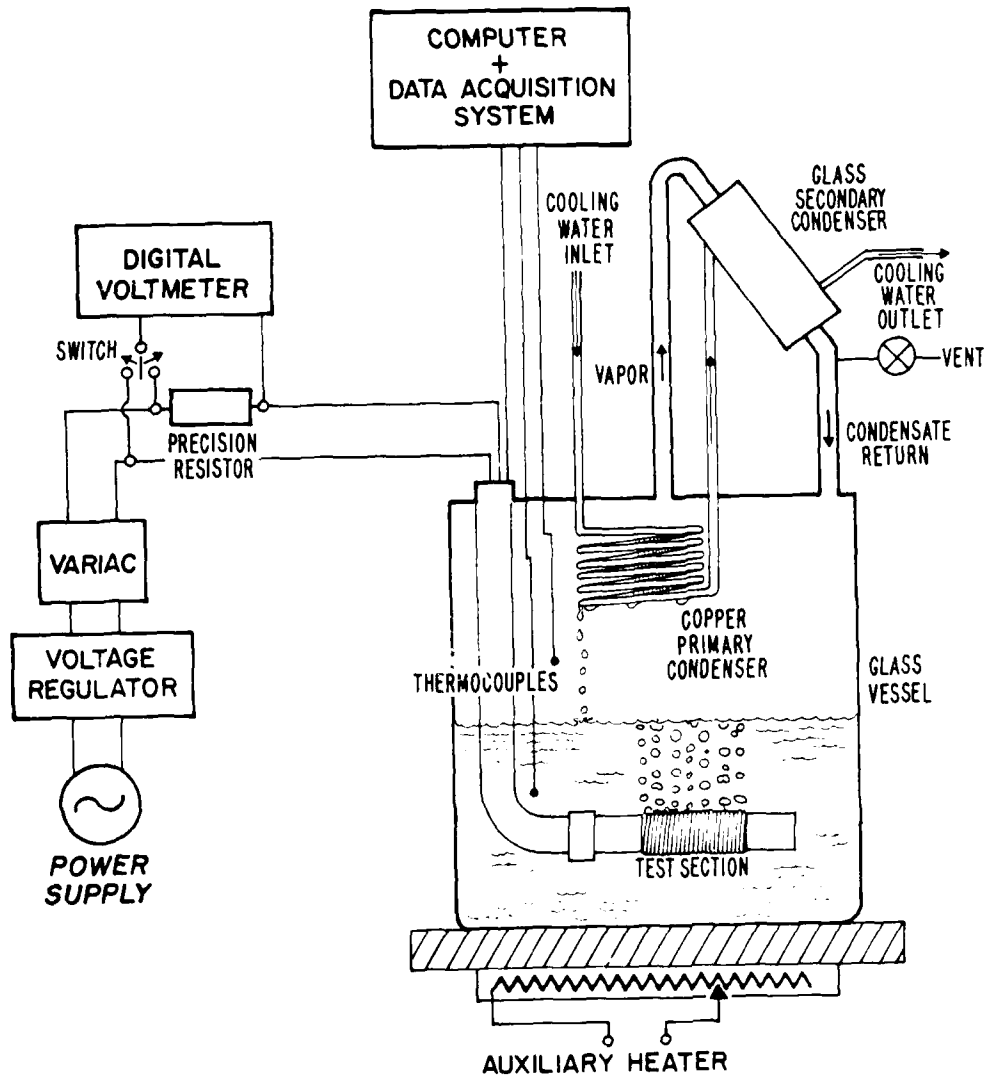


Figure 1. Schematic of Test Apparatus

Figure 1 shows a schematic of the test apparatus. The boiling surfaces consist of a cylindrical copper tube with a smooth interior surface and a commercially-available T-shaped finned surface manufactured by Wieland-Werke, AG. Each tube was conditioned for the insertion of thermocouples by drilling eight longitudinal holes as indicated in Figure 2 and introducing the respective copper-constantan thermocouples centered by means of capillary copper tubes. In the center of the tube a cartridge heater was placed to act as the heat source as shown in Figure 3.

Both ends of the test section were machined to remove the enhanced surface on the outside and to increase the interior diameter. This reduced the cross sectional area and thereby minimized the heat transfer from the ends of the test section. A Teflon plug was inserted into the free end for sealing and heat transfer reduction purposes. The other end of the test section was connected to a long copper extension tube through a 90-degree elbow, which allowed the test section to be placed in a horizontal position within a thick-walled Pyrex glass vessel. Since one of the requirements of the apparatus was to maintain the liquid at saturation temperature and atmospheric pressure, a plate heater and a vent tube were provided to satisfy these conditions. In addition avoiding excessive loss of vapor, a water-cooled copper coil was placed in the vapor space of the vessel, to act as a primary condenser. The vessel was covered with a

II. EXPERIMENTAL APPARATUS

A. REQUIREMENTS GOVERNING DESIGN

The purpose of this research was the observation of nucleate pool boiling from different Gewa-T surfaces. In order to get a more comprehensive knowledge about the physical mechanisms that govern this phenomenon, it is necessary to measure the parameters involved which affect the nucleate boiling process. The selected parameters to be obtained are the following:

1. Barometric pressure
2. Test section wall temperature
3. Fluid bulk temperature
4. Vapor temperature
5. Surface heat flux

B. TEST APPARATUS

The experimental apparatus designed by Lepere [Ref. 9], and modified by Hernandez [Ref. 8], with further minor modifications, was used during this thesis work. To gather data more conveniently at a faster rate, a Hewlett Packard model 9826 computer and an HP-3054A automatic data-acquisition system were added to the experimental facility. Lepere [Ref. 9] and Hernandez [Ref. 8] provide detailed descriptions of the apparatus; therefore, only a brief description is presented in this thesis.

to improve this performance through the use of further enhancing techniques.

There were four major objectives in this thesis study:

1. Take data to verify results of Hernandez [Ref. 8] on a standard 21.2 mm O.D. Gewa-T tube with and without shrouds.

2. Use wire wraps in the inter-fin area to improve nucleate-boiling heat-transfer performance from Gewa-T tubes.

3. Take data using the combination of best shroud (found in 1) and the best number of wire wraps (found in 2) on Gewa-T tubes.

4. Take data to study the effect of fin-tip spacing and fin density on the heat-transfer performance of Gewa-T tubes.

increase in the heat-transfer coefficient when compared to plain surface. The High Flux surface was most effective over a broad range of heat fluxes. The Thermoexcel-E surface showed similar gains in heat-transfer coefficient to that of the High Flux surface below 10 kW/m^2 . The Gewa-T surface was not as effective as the other surfaces at low heat fluxes but performed comparably at high heat fluxes (near 100 kW/m^2).

Marto and Hernandez [Ref. 7] studied the boiling performance of a Gewa-T finned surface in Freon-113. They examined the influence of placing aluminum shrouds around the test tubes, and found that the thermal performance of these surfaces were dependent upon the liquid-vapor flow within the channels between neighboring T-shaped fins. They also examined the influence of the fins by progressively machining away the fin height to arrive at a smooth cylindrical surface. They reported that the addition of the "T-caps" to straight fins produced the most significant improvement in heat-transfer performance when compared to a smooth tube. The use of shrouds increased the heat-transfer coefficient at all practical heat fluxes, but decreased the heat-transfer coefficient at very high heat fluxes when compared to the unshrouded surface.

B. THESIS OBJECTIVES

Based on the foregoing discussion, the major motivation in this work was to further study the boiling heat-transfer performance of Gewa-T surfaces in R-113, and to attempt

development of generalized correlations or successful theoretical models.

Yilmaz, et al. [Ref. 5] compared the nucleate pool-boiling heat-transfer performance of three copper tubes: Linde High Flux, Wieland Gewa-T and Hitachi Thermoexcel-E. Their data taken with p-xylene showed that while all tubes performed better than smooth tubes, the best performance was with the Linde High Flux surface. The Thermoexcel-E tube performed better than the Gewa-T tube at low heat flux and both performed similarly at high heat flux. These data were taken under the fully-established boiling regime; thus, no information was provided on the hysteresis behavior or temperature overshoot of these surfaces.

Bergles and Chyu [Ref. 6] compared the nucleate pool-boiling heat-transfer performance of four different Linde High Flux tubes to a plain copper tube in distilled water and in R-113. They used three different methods of aging the test surface prior to collecting data. They reported significant temperature overshoots of both plain and High Flux surfaces in R-113. They also reported that these overshoots were sensitive to aging, initial subcooling and rate of power increase.

Marto and Lepere [Ref. 1] obtained results on the heat-transfer performance of three heat-transfer surfaces: Linde High Flux, Thermoexcel-E, Gewa-T, and a plain copper surface in R-113 and FC-72. They reported a two to tenfold

Nishikawa and Ito [Ref. 4] recently discussed two methods to augment nucleate boiling: (1) use teflon-coated pits to reduce wettability of boiling liquid, and (2) manufacture surfaces with numerous re-entrant cavities that have the ability to trap vapor and keep the nucleation sites active. Due to the high wettability of low surface-tension fluids (such as fluorocarbons), the use of teflon-coated pits has not been successful. Thus, the surfaces with re-entrant-type cavities are the viable candidates for low surface-tension liquids.

Taking advantage of the concept of re-entrant cavities, a number of enhanced boiling surfaces have been invented during the last two decades. They include the Linde High Flux surface of Union Carbide, Gewa-T surface of Wieland and Thermoexcel-E surface of Hitachi. All of these surfaces are provided with re-entrant cavities through specialized manufacturing processes. These re-entrant cavities introduce yet more parameters to be desired.

In view of the inadequate understanding of the nucleate pool boiling process on smooth tubes, a thorough understanding of the boiling process on advanced surfaces may take many more years to come. Thus, present-day designers have very little information when considering advanced boiling surfaces. It is very important that researchers gather a vast amount of experimental data covering a wide range of heat-transfer fluids. Such extensive data will enable the

good indication of the complex nature of the nucleate boiling process. Chongrungron and Sauer [Ref. 2] summarized nine(9) correlations for nucleate pool boiling of single-component fluids from smooth tubes. They stated the inadequacy of any of these correlations when compared with experimental data.

Nucleate pool boiling is strongly dependent on the surface structure; i.e., the heat flux increases with increase in stable nucleation site density. The size, shape and density of such nucleation sites are almost impossible to predict. However, the entire nucleate pool-boiling process is dependent on the performance at these nucleation sites. It is well known that the ability of these sites to develop and trap small vapor bubbles is the reason for improved performance in nucleate pool boiling in comparison with natural-convective boiling.

When a bubble is being generated at a surface nucleation site (or a pore), the wall superheat is given by the following approximate theoretical equation [Ref. 3]:

$$T_W - T_S = \frac{2 \sigma T_S}{\rho_V h_{FG} R}$$

Thus, for a given fluid, the wall superheat can be decreased (boiler performance increases with decrease in wall superheat) with increase in pore radius. Of course, this radius must have a practical upper limit since too large a pore would not trap a vapor bubble.

I. INTRODUCTION

A. BACKGROUND

The energy crisis that began in 1974 has made a considerable impact on the design and operation of energy-conversion devices. Today, designers are challenged to design more and more efficient heat-transfer systems. Among the numerous areas that designers are faced with this challenge, boilers or evaporators used in many engineering applications demand considerable attention. The use of advanced boiling surfaces may lead to significant improvements in efficiency and/or significant savings in the initial cost and equipment sizes. Also, due to the ever-decreasing sizes of electronic components, the presence of very high heat fluxes has made the cooling of such components a challenging problem. Marto and Lepere [Ref. 1] stated that the use of advanced boiling surfaces may have potential promise in the field of electronic cooling. However, the lack of generalized performance data and useful theoretical models for such advanced surfaces have still kept designers away from the utmost use of these surfaces.

Due to a lack of complete understanding, the theoretical treatment of the nucleate pool-boiling process, even on a smooth surface, is extremely complex. The existence of a large number of semi-empirical formulas is probably a very

ACKNOWLEDGMENTS

Above all, the author must thank for the continuous encouragement he received from his wife.

For their infinite patience and accurate guidance throughout this investigation, the author is sincerely grateful to Dr. Paul Marto and Dr. A.S. Wanniarachchi.

For their cooperation in furnishing samples of Gewa-T tubing, the author wishes to thank Wieland Werke AG, West Germany.

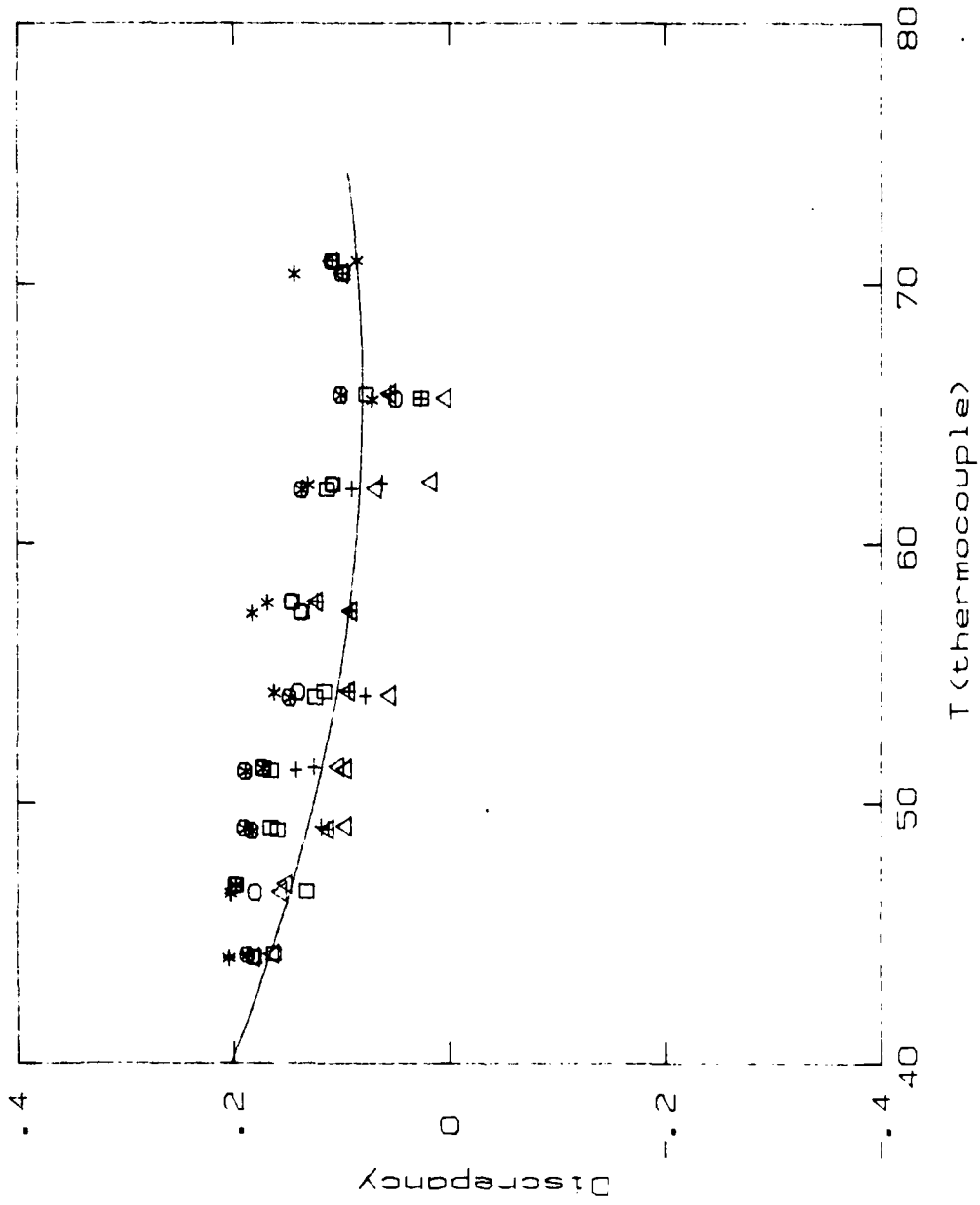


Figure 4. Thermocouple Calibration Curve

calibration line. Based on this fact, no calibration was performed for the other five tubes. Instead, the calibration curve generated for tubes 1 and 7 was assumed for all tubes.

III. EXPERIMENTAL PROCEDURES

A. NORMAL OPERATION

The Procedure B employed by Marto and Hernandez [Ref. 7] has been demonstrated to be the most adequate to carry out the boiling runs. Because of the large influence of surface past history on boiling incipience, this procedure was established to allow repeatability and permit comparison of the obtained data for different enhancements.

The procedure is as follows:

1. Once the test section has been immersed in the pool, it was subjected to one hour of pre-boiling by setting the cartridge heater to give a heat flux of about 30 kW/m^2 . The plate heater was adjusted to the maximum temperature for this one-hour period. This initial vigorous boiling served to degas the liquid and to force the noncondensable gases out to the atmosphere.
2. After the initial aging process, both test-section heater and plate heater were secured, allowing cooling of the liquid and the test section for about 30 minutes.
3. The plate-heater voltage was then adjusted in order to maintain the liquid at saturated conditions and the cartridge heater was turned on to the first setting of 12 volts.
4. For all the consecutive settings during both increasing and decreasing heat fluxes, the boiling was allowed to stabilize for five minutes at each power setting.

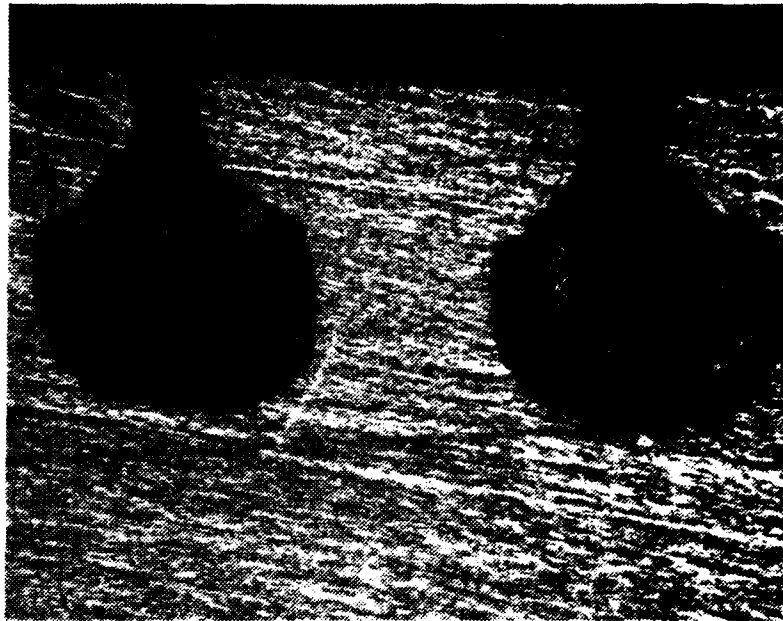
5. At a given power setting, the following data were recorded: heater voltage, precision-resistor voltage, vapor temperature, liquid bulk temperature and wall temperatures of the test section.

B. GEWA-T SURFACES

Three groups of surfaces were tested. The first surface was the same as used by Hernandez [Ref. 8] with a fin density of 0.75 fins/mm, an outside diameter of 21.2 mm, and an inter-fin gap of 0.25 mm. The second group of three tubes had 0.75 fins/mm, an outside diameter of 23.1 mm and inter-fin gaps of 0.15, 0.25 and 0.35, and the third group of three tubes had 1.02 fins/mm and all other specifications were the same as the second group.

The geometry of the enhancement of these seven Gewa-T surfaces was observed by making a longitudinal cut of the tubes and photographing them with 50X magnification (Figure 5). As can be seen, the tubes with 0.75 fins/mm had an approximately circular cavity shape, while the 1.02 fins/mm tubes had a somewhat elongated cavity shape. This difference in shape was probably due to the technique used in construction to obtain the various specifications. All the T-shaped fins had a fin height of approximately 0.95 mm.

The exact determination of diameters at the base of the fins was carried out from the magnified photographs of the cavities. This diameter was determined by subtracting twice the fin height from the measured outside diameter:



(a) Gewa-T Tube Number 2



(b) Gewa-T Tube Number 5

Figure 5. Optical Micrograph of Gewa-T Fin Profile, 50X

$$D_2 = \text{O.D.} - 2H_F ,$$

resulting in the dimensions presented in Table 1.

TABLE 1
Dimensions of Gewa-T Finned Tubes

TUBE NO.	FINS/ mm	FIN TIP GAP (mm)	FIN HEIGHT (mm)	O.D. (mm)	D ₂ (mm)
1	0.75	0.25	0.865	21.2	19.47
2	0.75	0.15	0.980	24.99	23.05
3	0.75	0.25	0.960	24.99	23.07
4	0.75	0.35	0.970	24.99	23.05
5	1.02	0.15	1.050	25.30	23.20
6	1.02	0.25	1.050	25.30	23.20
7	1.02	0.35	1.125	25.30	23.05

For simplicity, the diameter at the base (D₂) was assumed to be 19.5 mm for Tube 1 and 23.1 mm for all other tubes.

C. HEAT-FLUX CALCULATION

According to earlier description about test-section construction, the cartridge heater acts as the heat source, inserted into the tube, and variations in heat-transfer rate are made through different power settings with a variac.

$$Q_H = VI \quad (1)$$

where:

- Q_H = heat-transfer rate from the cartridge heater (W)
- V = voltage across the cartridge heater element (volts)
- I = current through the heater element (amps)

This circuit is connected in series with a precision resistor, which provides the means to compute the electrical current by the measurement of the voltage drop across the resistor:

$$I = V_{RES}/R \quad (2)$$

where:

- V_{RES} = voltage drop across the precision resistor (volts)
- R = resistance of the precision resistor (ohms)
= 2.031 ohms

Both ends of the Gewa-T tube were machined to provide a smooth surface and a reduced wall thickness in order to minimize longitudinal heat conduction and therefore the heat losses from the unenhanced ends. The geometry of these ends is shown in Figure 6, where:

- b = base of the T-shaped fins
- T_b = temperature at the base of T-shaped fins ($^{\circ}C$)

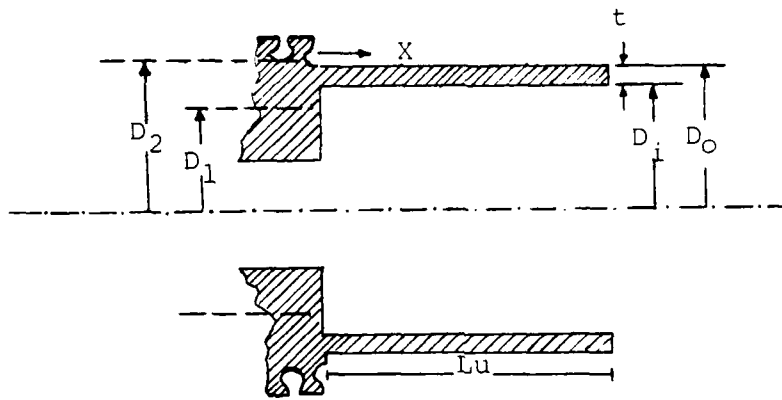


Figure 6. Geometry of Unenhanced Ends

For this cylindrical geometry:

$$A_C = \frac{\pi}{4}(D_O^2 - D_i^2) \quad (3)$$

$$A_S = P \times L_C \quad (4)$$

where:

A_C = cross-sectional area of tube wall (m^2)

D_O = tube outside diameter (m)

D_i = tube inside diameter (m)

A_S = tube outside surface area (m^2)

P = tube outside wall perimeter (m)

It was assumed that the temperature at the base of the thin-walled fin was equal to the temperature at the base of the T-shaped fins. Therefore:

$$\theta(x) = T(x) - T_{SAT} \quad (5)$$

In general,

$$\frac{d^2\theta}{dx^2} - m^2\theta = 0 \quad (6)$$

where:

$$m^2 = \frac{\bar{h} P}{kA_C} \quad (7)$$

Therefore

$$Q_F = Q_B = -kA_C \left. \frac{dT}{dx} \right|_{x=0} = -kA_C \left. \frac{d\theta}{dx} \right|_{x=0} \quad (8)$$

Now, assuming negligible convective heat loss from the thin tube tip:

$$\left. \frac{d\theta}{dx} \right|_{x=L_U} = 0 \quad (9)$$

and

$$\frac{\theta}{\theta_B} = \frac{\text{Cosh } m(L-x)}{\text{Cosh } mL} \quad (10)$$

For this case

$$Q_F = \sqrt{\bar{h} P k_C A_C} \theta_B \text{Tanh } mL_U \quad (11)$$

$$\theta_B = \theta(o) = T_B - T_{SAT} \quad (12)$$

where:

Q_F = heat-transfer rate through unenhanced end (W)

T_{SAT} = fluid saturation temperature ($^{\circ}C$)

k_C = thermal conductivity of the copper (W/m.K)

\bar{h} = average heat-transfer coefficient ($W/m^2.K$)

Assuming the wall temperature is the same as the average of the eight calibrated wall temperature thermocouple measurements, less temperature drop due to radial conduction from thermocouple position to the base of the T-shaped fin,

$$T_B = T_{AVG} - Q_H \frac{\ln(D_2/D_1)}{2 \pi L k_C} \quad (13)$$

$$T_{AVG} = \left(\sum_{n=1}^8 T_n \right) / 8.0 \quad (14)$$

where:

D_1 = diameter at the position of thermocouples (m)

T_{AVG} = average wall temperature ($^{\circ}C$)

For the geometry shown in Figure 6:

$$L_C = L_U + \frac{t}{2} \quad (15)$$

$$t = D_o - D_i \quad (16)$$

where:

L_C = corrected length (m)

L_U = length of unenhanced ends (m)

t = tube thickness (m)

The average difference between the wall temperature and the saturation temperature may now be determined from the following equation:

$$\bar{\theta} = \frac{1}{L_C} \int_0^{L_C} \frac{\text{Cosh } m(L_C - x)}{\text{Cosh } mL_C} dx \quad (17)$$

$$\bar{\theta} = \frac{\theta_B}{mL_C} \text{Tanh } mL_C \quad (18)$$

$$\bar{\theta} = \bar{T}_W - T_{SAT} \quad (19)$$

where:

$(T_W - T_{SAT})$ = average difference between surface wall temperature and fluid saturation temperature (K)

Since the unenhanced ends are very long and the thickness is very small, only very little heat transfer would take place at these ends. Thus, these ends undergo free convection,

for which the Churchill and Chu correlation as stated in [Ref. 10] for the average Nusselt number was assumed:

$$\text{Nu}_{D_o} = \left\{ 0.60 + \frac{0.387 \bar{Ra}_{D_o}^{1/6}}{[1 + (0.559/\text{Pr})^{9/16}]^{8/27}} \right\}^2 \quad (20)$$

$$10^{-5} < \bar{Ra}_{D_o} < 10^{12}$$

The average Nusselt number is:

$$\bar{Nu}_{D_o} = \frac{\bar{h} D_o}{k} \quad (21)$$

where:

k = thermal conductivity of Freon-113 (W/m.K)

Solving for h :

$$\bar{h} = \frac{k}{D_o} \left\{ 0.60 + \frac{0.387 \bar{Ra}_{D_o}^{1/6}}{[1 + (0.559/\text{Pr})^{9/16}]^{8/27}} \right\}^2 \quad (22)$$

$$\text{Pr} = \frac{\nu}{\alpha} \quad (23)$$

$$\bar{Ra}_{D_o} = \frac{g \beta (T_w - T_{SAT}) D_o^2}{\nu \alpha} \quad (24)$$

$$\beta = - \frac{1}{\delta} \frac{\Delta \rho}{\Delta T} \quad (25)$$

where:

- Pr = Prandtl number
- ν = kinematic viscosity (m^2/s)
- α = thermal diffusivity (m^2/s)
- \bar{Ra}_{D_o} = average Rayleigh number
- g = gravitational acceleration (m/s^2)
- β = volumetric thermal expansion coefficient ($1/K$)
- ρ = density of freon-113 (kg/m^3)

Now, substitution of Equations 7, 18 and 24 into Equation 22 results in:

$$\bar{h} = \frac{k}{D_o} \left\{ 0.60 + \frac{0.387 \left[\frac{g \beta D_o^3 \rho \tanh\left(\frac{\bar{h} P}{k A_C}\right) L_C^{1/2}}{\nu L_C \left(\frac{\bar{h} P}{k A_C}\right)^{1/2}} \right]^{1/6}}{[1 + (0.559/Pr)^{9/16}]^{8/27}} \right\}^2 \quad (26)$$

Equation 26 is solved for \bar{h} by iterative technique within a range of precision of 0.001. Knowing the value of natural-convective heat-transfer coefficient at unenhanced ends, the total heat-loss rate is calculated from Equation 11, and the heat-transfer rate through the enhanced Gewa-T surface is obtained by subtracting the total heat-loss rate from the total heat-transfer rate:

$$Q_{LOSS} = 2Q_F \quad (27)$$

$$Q = Q_H - 2Q_F \quad (28)$$

Finally, the heat flux from the Gewa-T surface at the base of the T-shaped fins is:

$$q = Q/A_B \quad (29)$$

$$A_B = \pi D_2 L \quad (30)$$

diameter. For this purpose, a semi-empirical correlation developed by Cornwell et al. [Ref. 11] is used:

$$Nu_{TB} = C_{TB} Re_{TB}^{2/3}$$

$$\frac{h_{TB} D}{k_F} = C_{TB} \left(\frac{qD}{h_{FG} \mu_F} \right)^{2/3}$$

$$\frac{k_F D V A}{\mu_F A} = \frac{\dot{m} D}{\mu_F A} = \frac{GD}{\mu_F}, \quad G = q/h_{FG}$$

$$h_{TB} = \frac{C_{TB} k_F}{D} \left(\frac{h_{TB} \Delta T D}{h_{FG} \mu_F} \right)^{2/3}$$

$$h_{TB}^{1/3} = \frac{C_{TB} k_F}{D} \left(\frac{\Delta T D}{h_{FG} \mu_F} \right)^{2/3}$$

$$h_{TB} = \left(\frac{C_{TB} k_F}{D} \right)^3 \left(\frac{\Delta T D}{h_{FG} \mu_F} \right)^2$$

$$h_{TB} = (C_{TB} k_F)^3 \left(\frac{\Delta T}{h_{FG} \mu_F} \right)^2 \frac{1}{D}$$

Using this relationship, Hernandez's data were revised and a least-squares-fit curve was generated. This curve is also plotted in Figure 12.

H. BOILING PERFORMANCE OF GEWA-T TUBE WITH SHROUDS

The same four shrouds tested by Hernandez were used during this investigation. These shrouds had the following geometry:

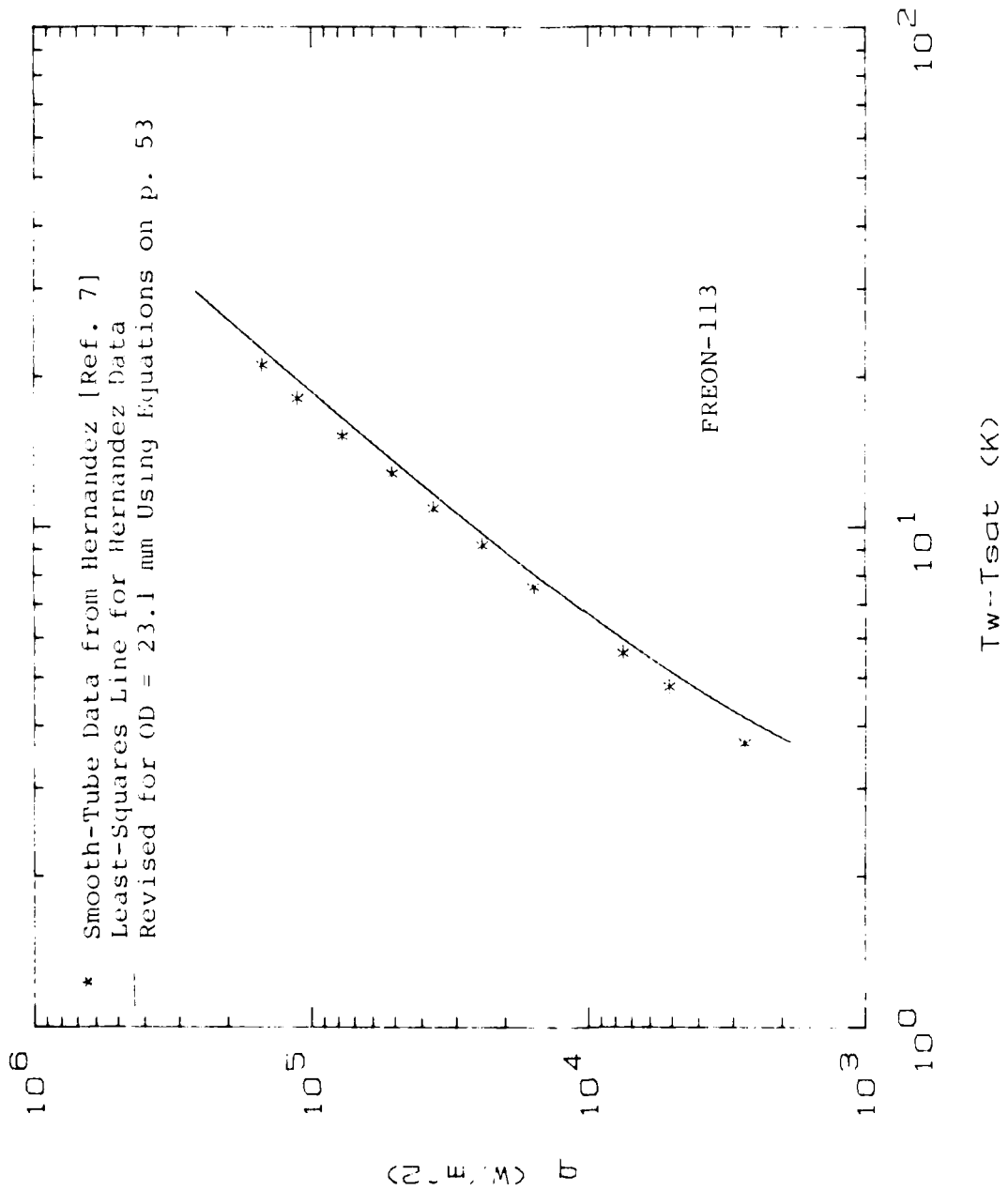


Figure 12. Extrapolation to Smooth Tube (23.1 mm OD) from Smooth-Tube Data of Hernandez (19.61 mm OD)

agree to within 0.2 percent at a heat flux of 30,000 to 100,000 W/m². These data runs show considerably good repeatability of this experiment. (Similar agreements were also found for all other tubes.)

Also, these data show a considerable enhancement of Gewa-T tube performance over the "Smooth" tube data of Hernandez. For example, at $\Delta T = 3.1$ K, the Gewa-T tube gives a 4.65 times larger heat flux than the smooth tube.

As also discussed by Lepere [Ref. 9] and Hernandez [Ref. 8] this enhancement in boiling performance is mainly attributed to the existence of re-entrant cavities in the Gewa-T tube.

G. BOILING PERFORMANCE OF SMOOTH TUBE

To compare the performance of Gewa-T tubes to smooth-tube performance, data of Hernandez were chosen. It is important to point out that his smooth tube did not consist of a commercially-available surface. Instead, Hernandez obtained his "Smooth" surface by machining fins off of a Gewa-T tube. He did not remove fins completely; the remaining portions on the tube measured about 0.1 mm.

Figure 12 shows Hernandez's data (heat flux as a function of wall superheat) for only decreasing heat fluxes. A least-squares-fit curve generated for these data points will be used in future figures representing data on tube 1. Since tubes 2 through 7 have a larger diameter, it was necessary to revise Hernandez's data to include the difference in

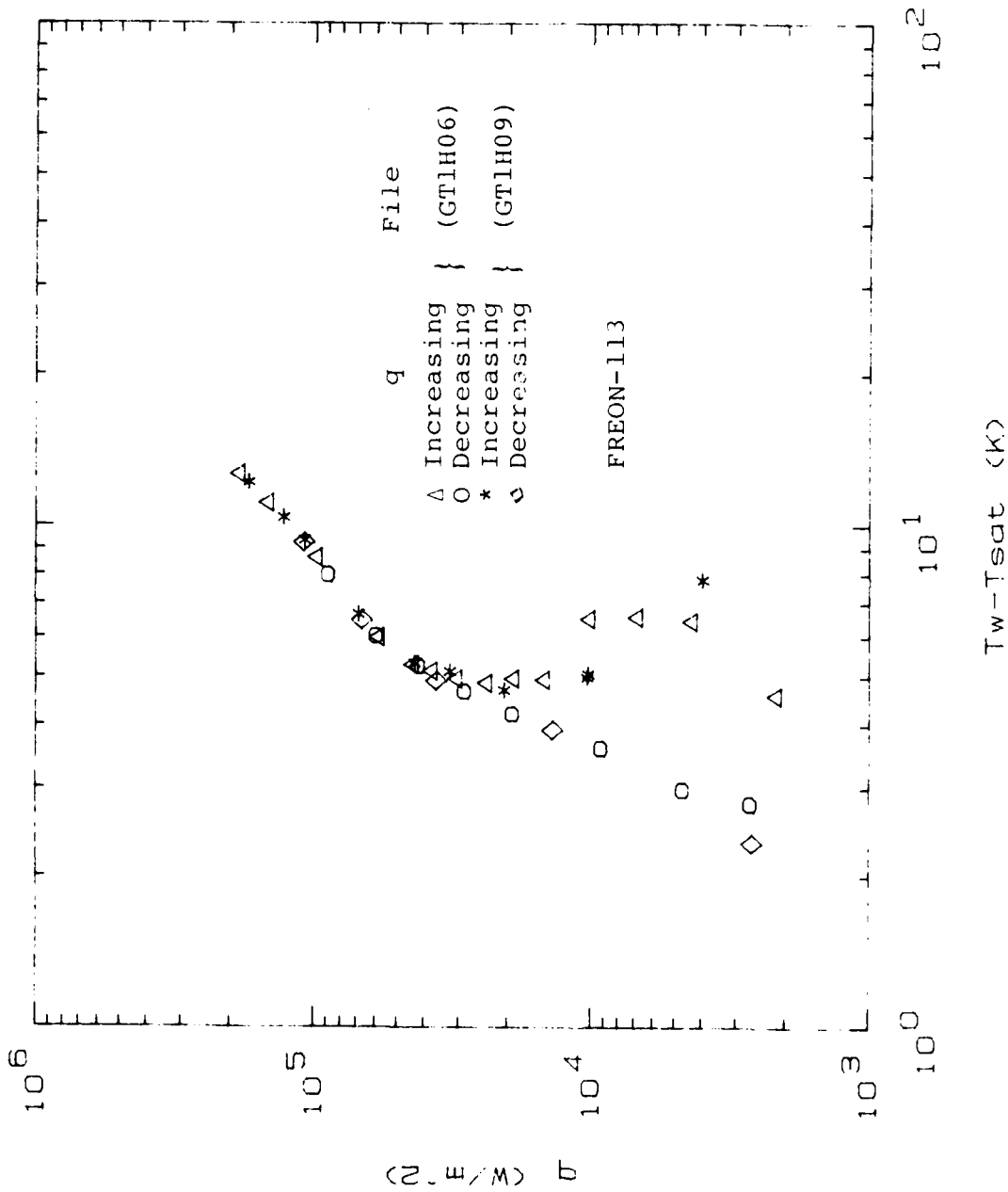


Figure 11. Reproducibility Test: Plain Gewa-T Tube 1

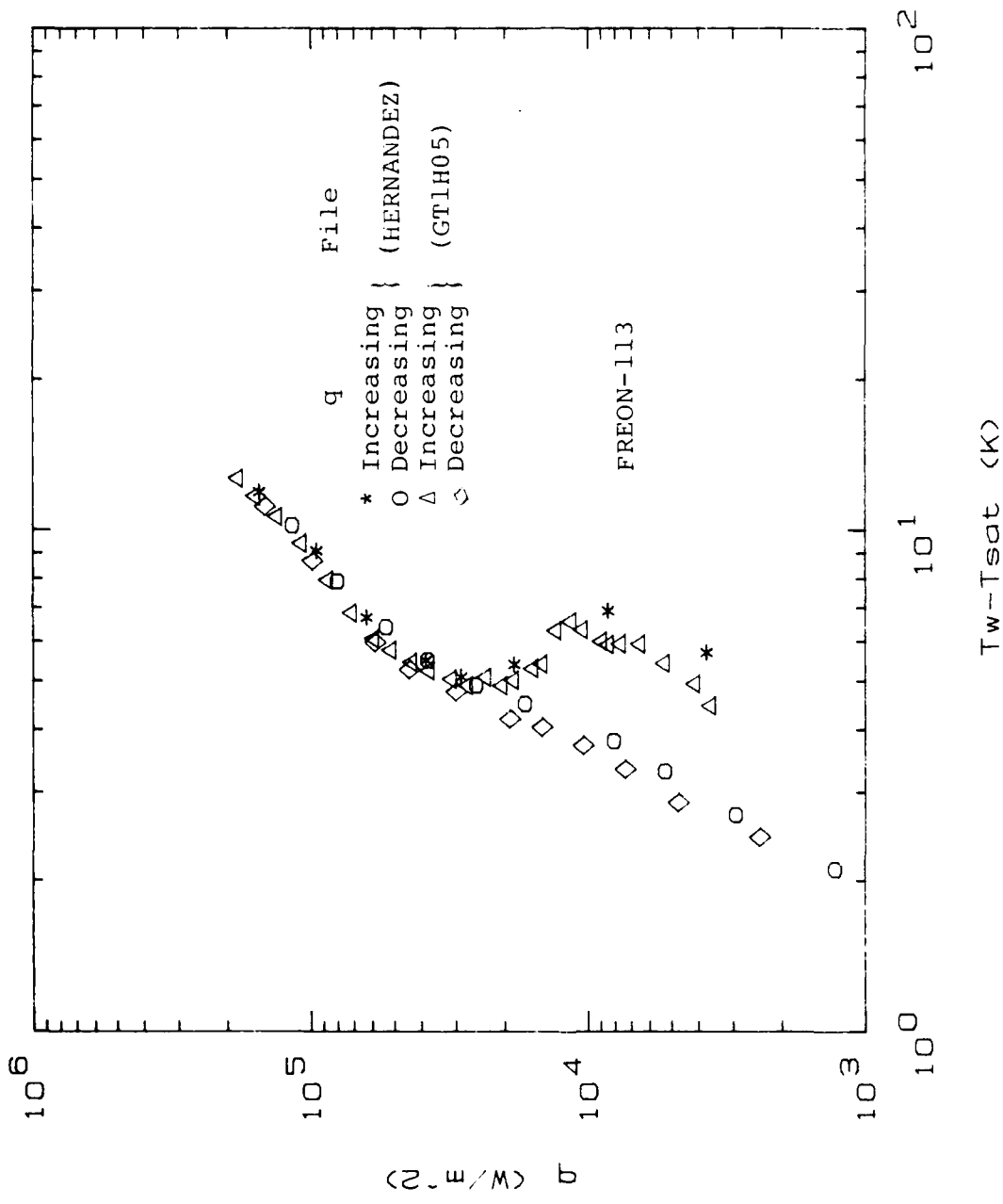


Figure 10. Reproducibility Test: Hernandez Run No. 3 Versus Present Work (GT1H05)

E. REPEATABILITY WITH PREVIOUS DATA

Following modifications made, especially to the data gathering means (i.e., automatic data-acquisition system and newly-written computer programs), it was necessary to take data for tube 1 (this is the same tube tested by Hernandez) to check the present data with Hernandez data under similar conditions. Even though a total of 5 different runs were made during this stage through debugging of programs and system familiarization, only run number 5 will be presented in this thesis with a comparison to Hernandez data.

Figure 10 shows the comparison between the present data and the data of Hernandez. A very good agreement is evident as the two sets disagree by less than 2 percent for the nucleate boiling regime. However, considerable disagreement exists in the region of increasing heat flux before total nucleate boiling. This is believed to be due to the rather random behavior of the boiling process during this regime as it will be presented in the next section, even two consecutive runs for a given tube would not give the same results during the unstable boiling regime.

F. REPEATABILITY STUDY OF PRESENT WORK

Figure 11 shows data from two different runs completed on two different days. As discussed earlier, a considerable disagreement can be seen before the tube undergoes complete nucleate-boiling process. However, for the complete nucleate-boiling process, the data from different data runs

confirmed the validity of the mathematical model assumed for data reduction. However, a small rate of bubble formation was evident at the tip of the unenhanced fin end; these bubbles were in fact generated at the base of the fin (i.e., between the Teflon plug and the inner surface of the fin).

The vapor bubbles generated in the inter-fin cavities are carried up into the channels around the tube due to buoyancy forces. As these bubbles travel up, they activate more and more nucleation sites as well as they help for the removal of larger bubbles from the channels. This phenomenon is generally referred to as the "Chimney Effect."

If the heat flux is too large (see Figure 7), the rate of vapor bubble generation may be too large that the interfin channels could be full of a vapor blanket that may disrupt the flow of liquid to the hot metal surface where active boiling takes places. At this point, further increase in heat flux may result in excessive wall temperatures. Under these conditions, vapor bubbles were seen ejecting radially outward from the test surface. Line D-E represents the boiling regime just described. It is clear that the slope (i.e., heat-transfer coefficient) at E is considerably smaller than that at point D. This decrease in heat-transfer coefficient is assumed to be due to the existence of an insulating vapor blanket.

When heat flux is gradually decreased, the curve follows a different path (D-F) as shown in Figure 7. This is due to the existence of stable nucleation sites that will remain active for a wide range of heat fluxes.

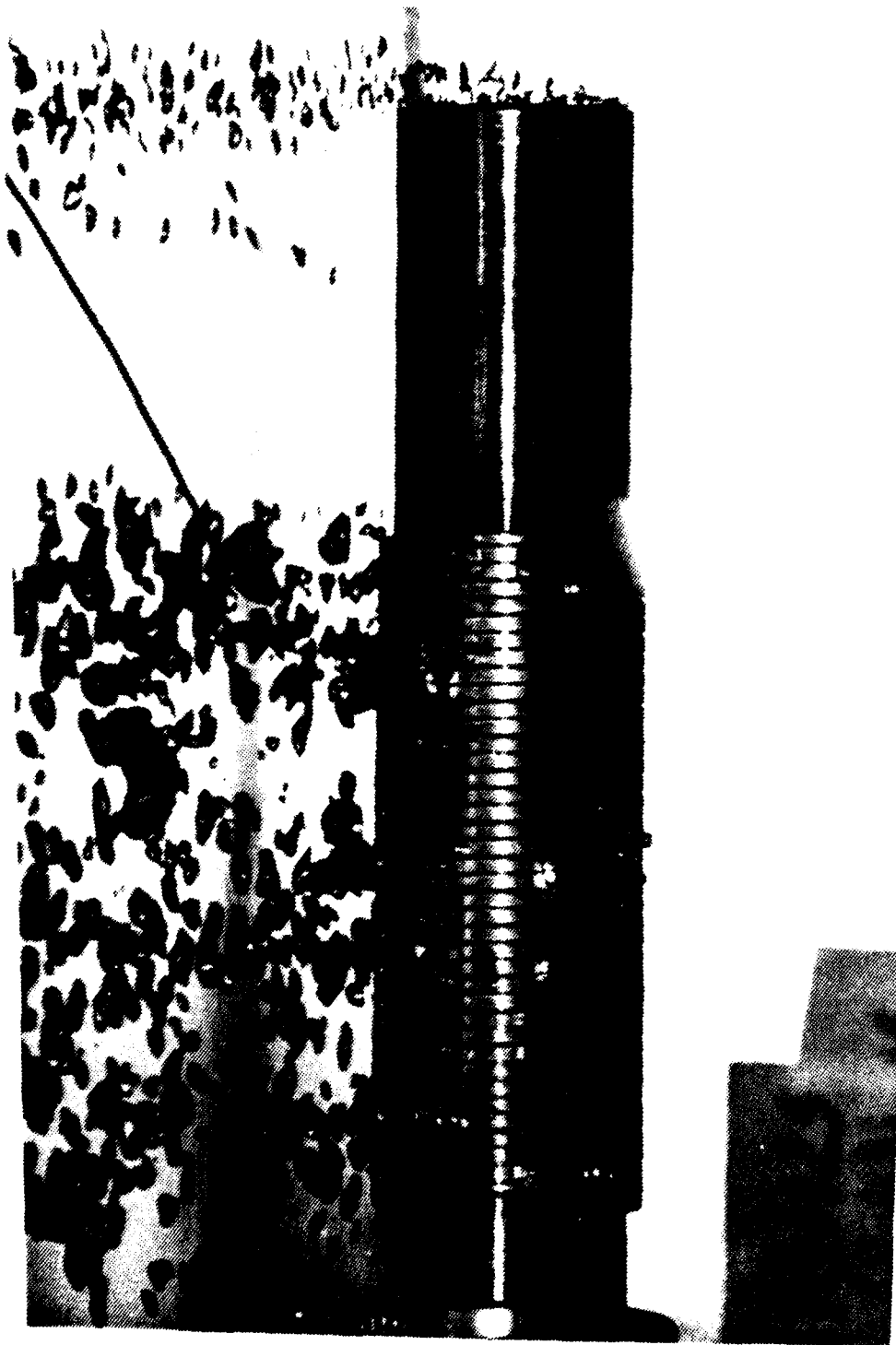


Figure 9. Photograph of Gewa-T Surface at Low Heat Flux

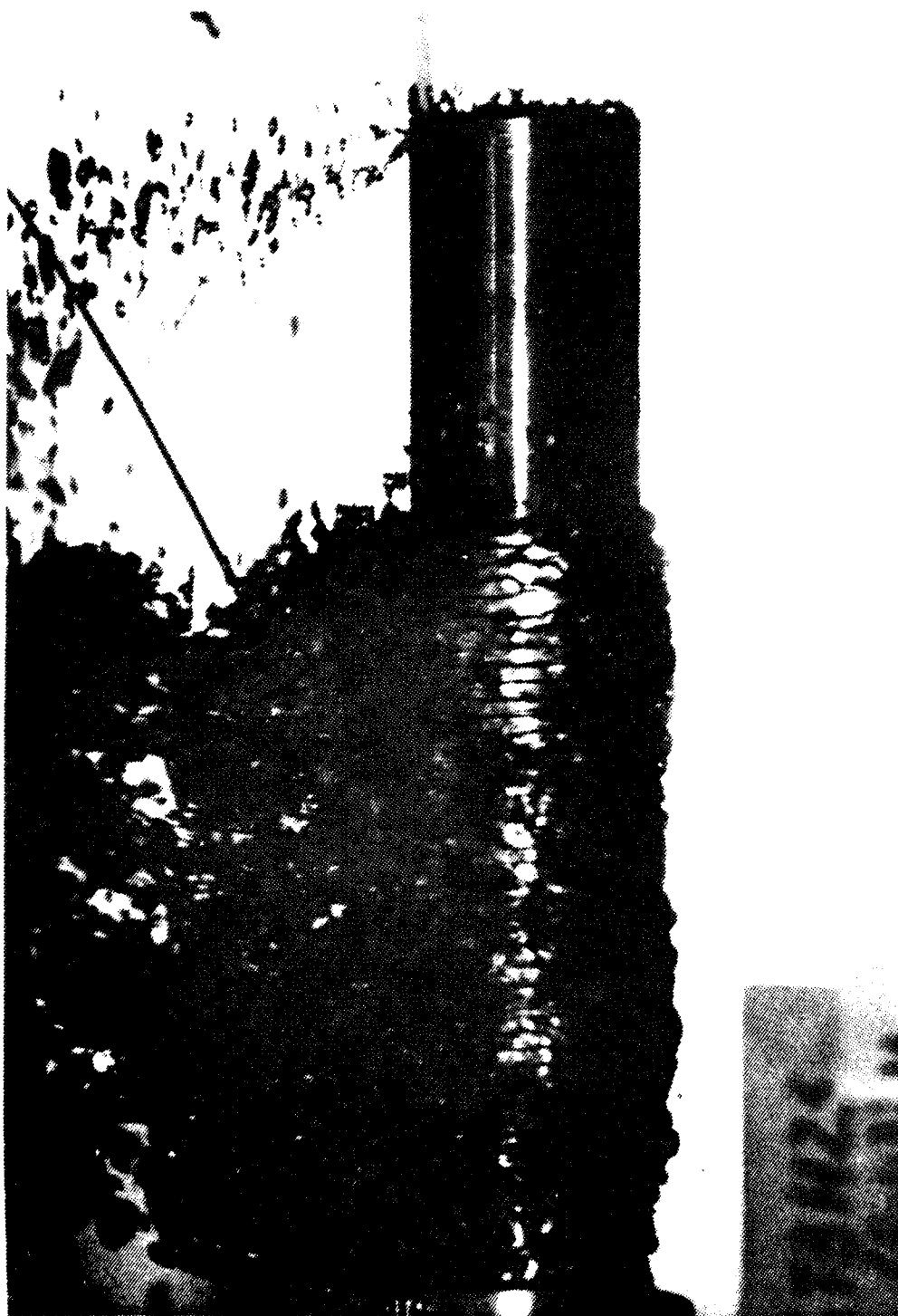


Figure 8. Photograph of Gewa-T Surface at High Heat Flux

From point A to point B, a continuous increase in heat flux, accompanied by an increase in wall superheat ($T_W - T_{SAT}$) is observed when heat flux is increased. This region corresponds to natural-convection process, as also verified during experimental runs with the absence of bubbles along both enhanced surface and unenhanced ends.

From point B to point C, a drastic reduction in wall superheat was observed while the heat flux continuously increased. This region was somewhat unstable as more and more nucleation sites became active. This region is known as the mixed boiling region, where transition from natural-convective boiling to nucleate pool boiling takes place. At these heat fluxes, visual observations revealed that the bubble formation was quite random. While some portions of the tube showed bubbles, other portions showed no bubble formation. The wall superheat continued to decrease until all nucleation sites became active, as indicated by point D.

Once all available nucleation sites have been activated, the wall superheat starts to increase with increasing heat flux as shown by region D to E. When boiling in this region, the entire tube showed very high density of bubble formation. At this point, it is important to point out that during all experimental runs, for the entire range of power settings (7.5 to 485 W), little or no nucleate pool boiling on the unenhanced surface of the ends was observed (see Figures 8 and 9) for the different test sections tested. This observation

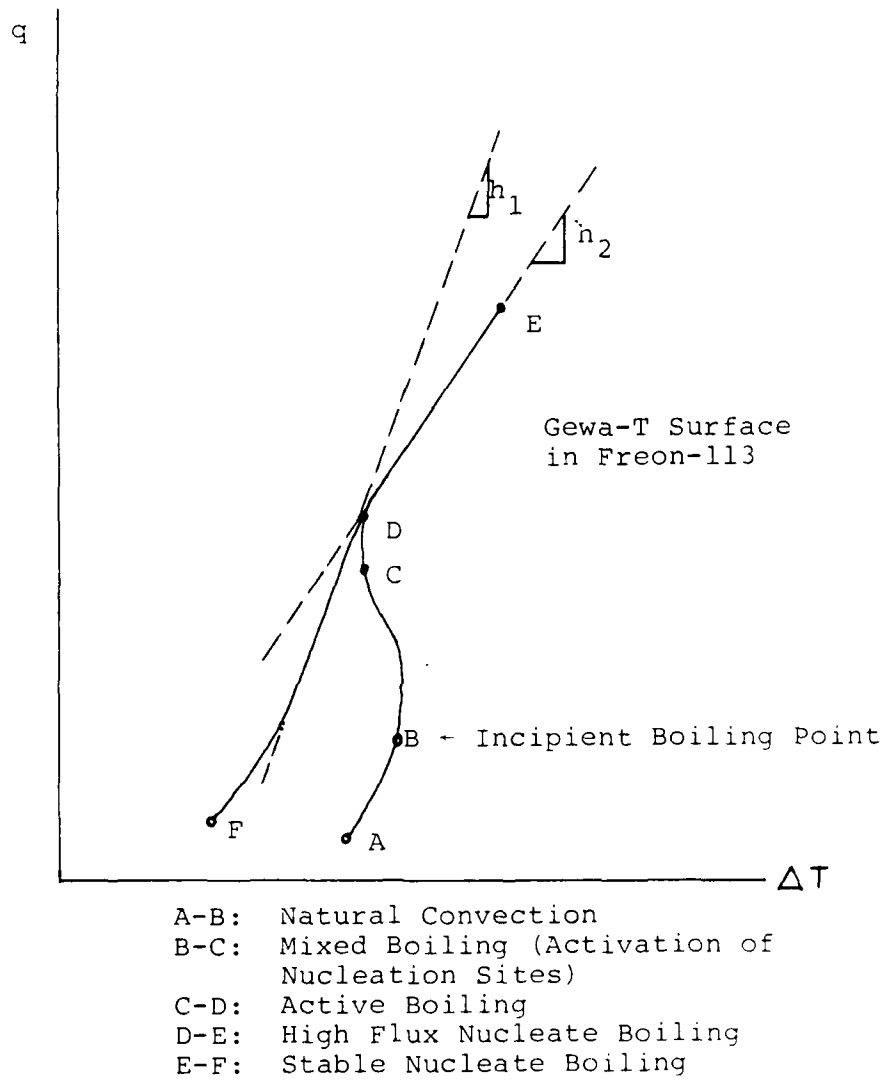


Figure 7. Typical Nucleate Pool-Boiling Curve
 for a Gewa-T Surface

runs were made. All of these runs showed only a negligible variation of the wall thermocouple temperatures; maximum variation was ± 0.25 K. These runs clearly showed that the heater element indeed provided a uniform heat flux along the circumferential direction. No detailed data are presented in this thesis for the tube in the vertical position. All other results presented herein are for the tubes in the horizontal position.

C. LONGITUDINAL UNIFORMITY OF HEAT FLUX ALONG THE TEST SECTION

During most of the data runs with the tubes in the horizontal position, somewhat unexplainable phenomena were observed. As the heat flux was gradually increased, bubble formation began simultaneously at the two ends, while the center portion of the tube underwent only natural convection. Approximately 40 percent of maximum heat flux was necessary to obtain nucleate boiling from the entire tube. Since all the wall thermocouples are located at midway along the tube, the average wall temperature values provided in all data runs may be in slight error.

D. PLOT ANALYSIS FOR PLAIN SURFACE

Figure 7 represents a typical curve for nucleate pool-boiling process of Gewa-T surface in Freon-113. The observed behavior of this process is analyzed in this section by studying the different sections of the boiling curve.

separate file. This plot data file could easily be recognized by the "P" added at the beginning of the raw data file name. In this manner, the plot data file corresponding to the above raw data file has the name PGT5H28.

A total of thirty different data runs were carried out during this investigation. These runs break down in the following manner:

<u>Run Number</u>	<u>Tube Number</u>	<u>Test Condition</u>
1 - 3	1	Plain - Vertical position
4 - 10	1	Plain - Horizontal
11 - 21	1	With shrouds and/or Wires
22 - 23	2	Plain - Horizontal
24 - 25	3	Plain - Horizontal
26	4	Plain - Horizontal
27 - 28	5	Plain - Horizontal
29	6	Plain - Horizontal
30	7	Plain - Horizontal

B. CIRCUMFERENTIAL UNIFORMITY OF HEAT FLUX AROUND HEATER ELEMENT

During the early stages of this investigation, it was thought necessary to test if the heater element would provide a non-uniform heat flux along the circumferential direction. Such a non-uniform heat-flux variation was assumed possible based on the heater-element construction. Therefore, tube 1 was immersed vertically in the R-113 liquid pool and three

IV. RESULTS AND DISCUSSION

A. DESIGNATION OF DATA FILES

A total of seven Gewa-T tubes were tested during this investigation. As can be seen from Table 1, the primary geometric variables were: fin-tip gap, fin density and outside diameter of tubes including fins.

The general designation for data files is:

GTNPnn

where:

- GT indicates Gewa-T surface
- N specifies the number of the tube tested (Table 1)
- P indicates the position of the test section (i.e., H for horizontal and V for vertical), and
- nn indicates the corresponding cumulative run number.

For example, GT5H28 specifies tube number five tested in the horizontal position during run number 28. From Table 1, the corresponding specifications for this test section are: 25.3 mm outside diameter, 23.1 mm diameter at the base of the fins, 1.02 fins/mm and inter-fin gap of 0.15 mm. While the file name just presented contain data in the very raw form, the processed data (i.e., q versus ΔT) were stored in a

<u>Shroud Number</u>	<u>Upper Opening</u>	<u>Lower Opening</u>
1	60°	60°
2	60°	30°
3	30°	30°
4	60°	8.5°

All of these shrouds had been designed for tube 1; thus, no shrouds were used for tubes 2 through 7.

Figures 13, 14, 15, and 16 show data on tube 1 with shroud numbers 1, 2, 3 and 4, respectively. As also reported by Hernandez [Ref. 8], all the shrouds improved boiling performance at low heat fluxes compared to plain Gewa-T tube. Table 2 lists performance calculations for tube 1 with various shrouds. It can be seen that the 60° × 8.5° shroud (number 4) produced the maximum improvement of 253 percent in the boiling coefficient over smooth tube at a heat flux of 10,000 W/m². At this heat flux, the 30° × 30° shroud resulted in a 165 percent improvement in the boiling heat-transfer coefficient. At a heat flux of 50,000 W/m², all shrouds resulted in about 190 percent improvement, except the 30° × 30° shroud which resulted in a 180 percent improvement.

At very high heat fluxes, for example at $q = 100,000 \text{ W/m}^2$, the 60° × 60° shroud showed a maximum performance increase of 106 percent; the 60° × 30° shroud resulted in a 49 percent improvement; the 60° × 8.5° shroud resulted in a 18 percent increase; and the 30° × 30° shroud resulted in an 13 percent

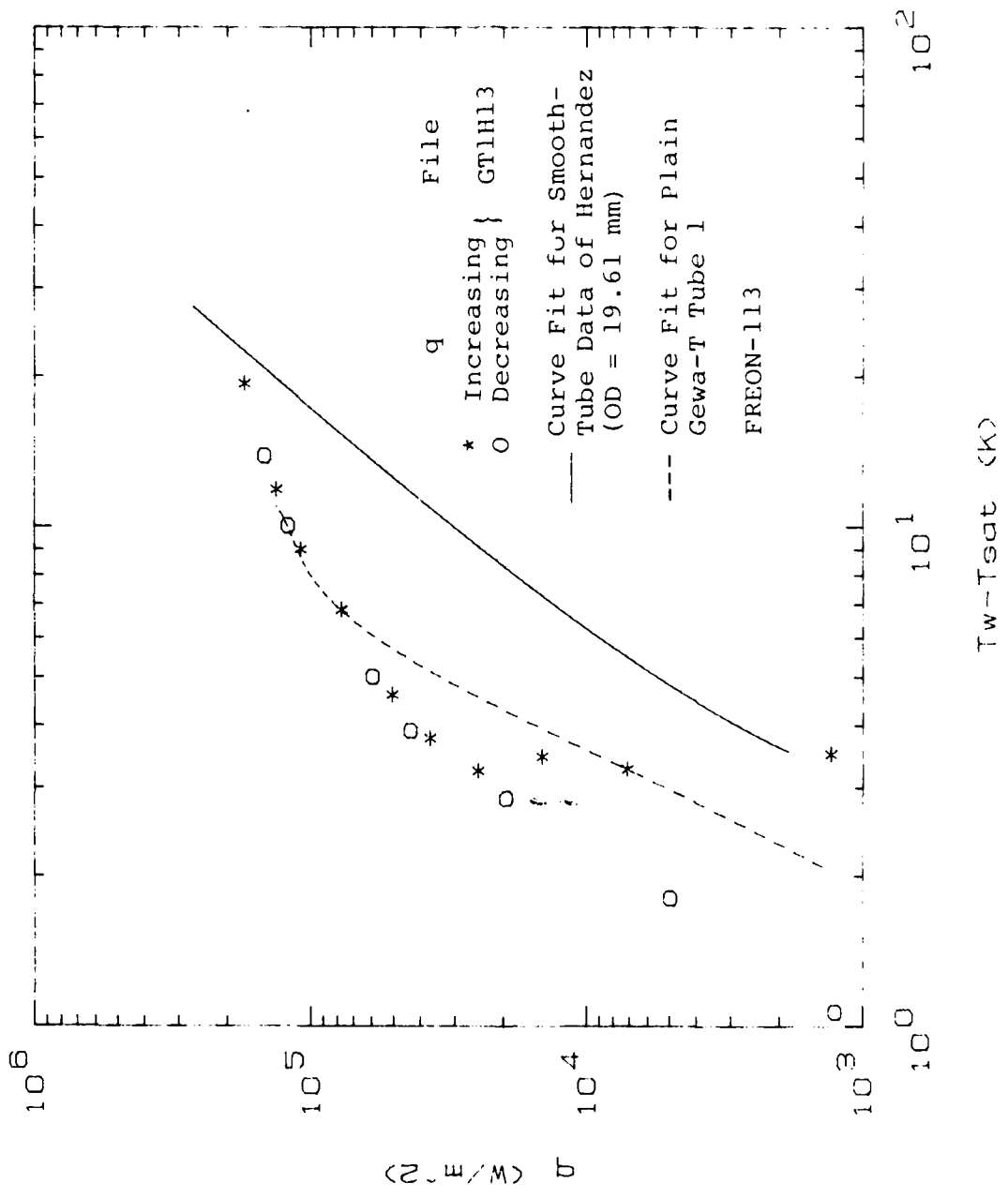


Figure 13. Effect of 60° x 60° Shroud on Boiling Performance of Plain Gewa-T Tube 1

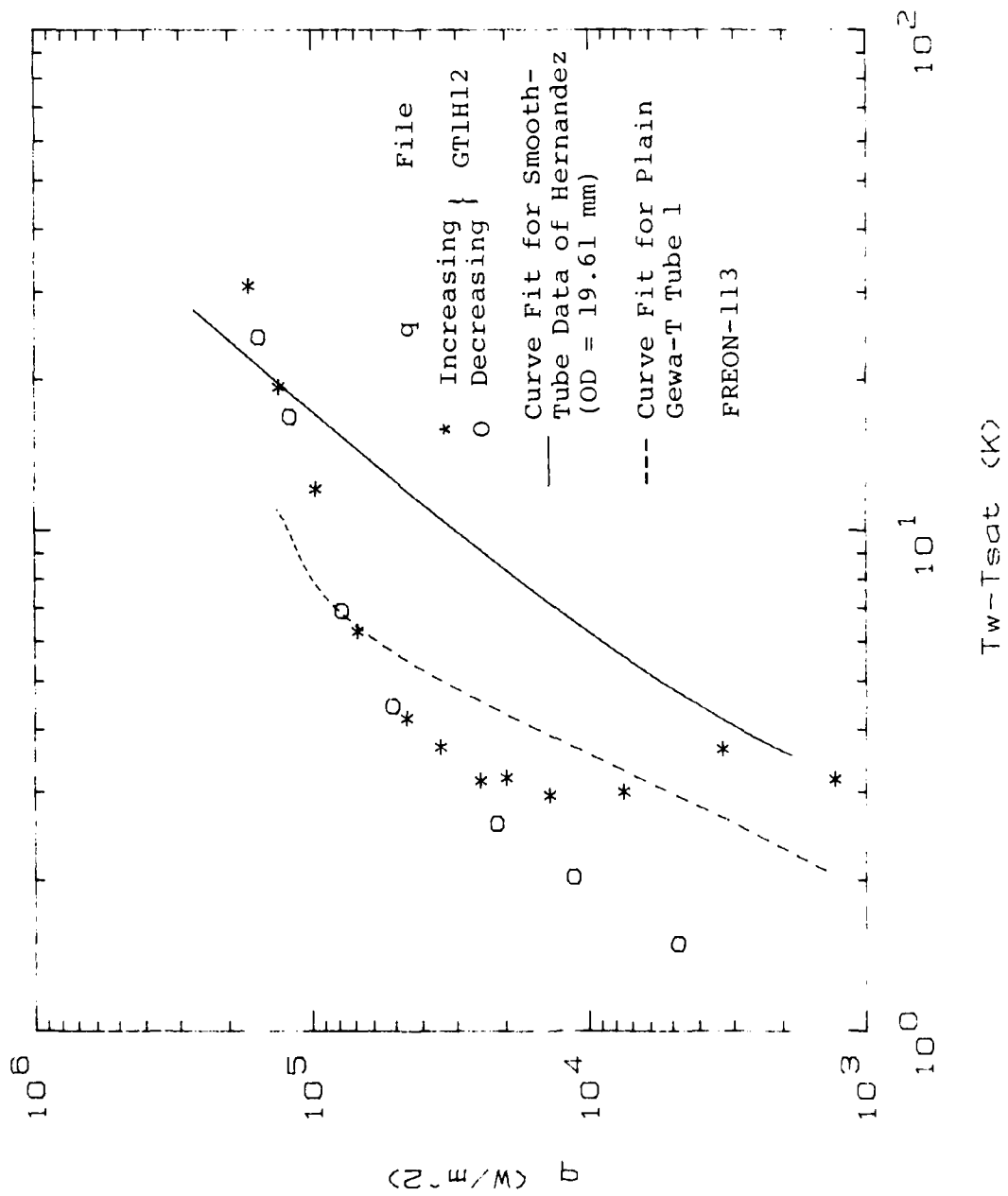


Figure 14. Effect of 60° x 30° Shroud on Boiling Performance of Plain Gewa-T Tube 1

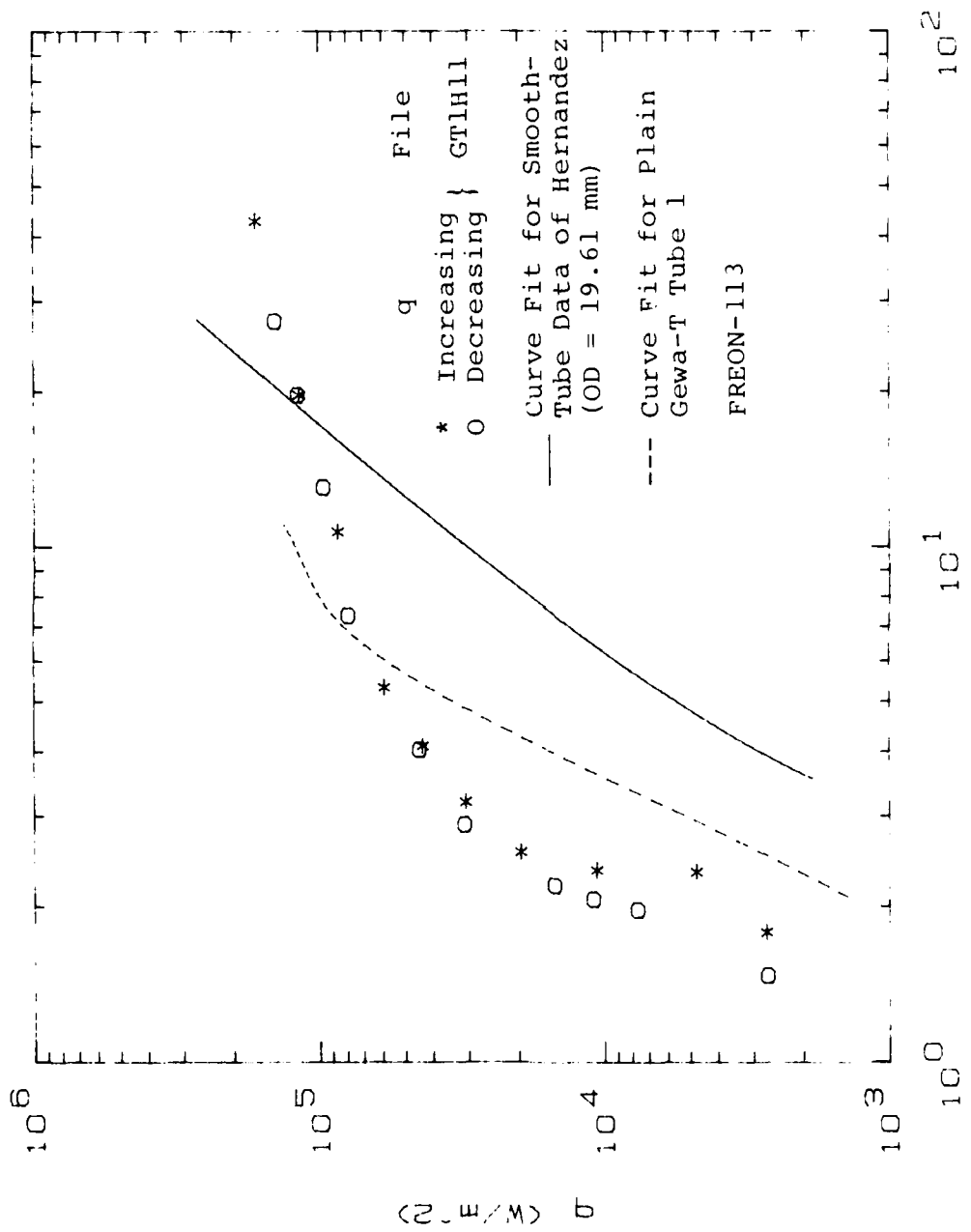


Figure 16. Effect of 60° x 8.5° Shroud on Plain Gewa-T Tube 1

TABLE 2

Summary of Results

DATA FILE NAME	TEST CONDITION	q = 10,000 W/m ²			q = 50,000 W/m ²			q = 100,000 W/m ²		
		ΔT (°C)	h (W/m ² -K)	% INCR.	ΔT (°C)	h (W/m ² -K)	% INCR.	ΔT (°C)	h (W/m ² -K)	% INCR.
HERNANDEZ	SMOOTH	6.22	1607.7	-	12.7	3937.0	-	17.0	5882.4	-
GT1H05	PLAIN	3.68	2717.4	69.0	5.55	9009.0	128.8	8.77	11,402.5	93.8
GT1H09	PLAIN	3.65	2739.7	70.4	5.65	8849.6	124.8	8.61	11,614.4	97.4
GT1H11	Shrd. 60x8.5	1.76	5681.8	253.4	4.36	11,467.9	191.3	14.38	6954.1	18.20
GT1H12	Shrd. 60x30	1.94	5154.6	220.6	4.42	11,312.2	187.3	11.39	8779.6	49.30
GT1H13	Shrd. 60x60	2.50	4000.0	148.8	4.37	11,441.7	190.6	8.26	12,106.5	105.8
GT1H21	Shrd. 30x30	2.35	4255.3	164.7	4.54	11,013.2	179.7	15.07	6635.7	12.8
GT1H14	2 WIRES	2.25	4444.4	176.4	4.86	10,288.1	161.3	7.68	13,020.8	121.4
GT1H16	3 WIRES	1.41	7092.2	341.1	4.33	11,547.3	193.3	7.38	13,550.1	130.4
GT1H17	4 WIRES	1.58	6329.1	293.7	4.62	10,822.5	174.9	7.32	13,661.2	132.2
GT1H18	5 WIRES	1.62	6172.8	283.1	4.39	11,389.5	189.3	7.01	14,265.3	142.5
GT1H19	3 WR-Shr 60x8.5	1.07	9345.8	481.3	4.47	11,185.7	184.1	17.37	5757.1	-2.1
EXTRAPO- LATION	SMOOTH	6.57	1522.1	-	13.56	3687.3	-	18.55	5390.8	-
GT2H22	PLAIN	4.52	2212.4	45.4	6.94	7204.6	83.0	8.91	11,223.3	108.2
GT3H25	PLAIN	3.65	2739.8	80.0	6.12	8169.9	107.5	9.53	10,493.2	94.7
GT4H26	PLAIN	4.66	2145.9	41.0	8.34	5995.2	52.3	11.44	8441.3	62.2
GT5H27	PLAIN	5.13	1949.3	28.1	7.44	6720.4	70.7	9.38	10,661.0	97.8
GT5H28	PLAIN	5.15	1941.8	27.6	7.51	6605.0	67.8	9.56	10,460.3	94.0
GT5H29	PLAIN	3.24	3086.4	102.8	6.02	8305.7	111.0	8.5	11,764.7	118.2
GT7H30	PLAIN	5.18	1930.5	26.8	8.35	5988.0	52.1	10.61	9425.1	74.8

improvement. It can be seen that the values just presented are somewhat proportional to the summation of the two shroud angles. This behavior indicates that at very high heat fluxes, too small a shroud opening can obstruct the outflow of vapor and/or the inflow of liquid.

However, it must be noted that at all practical heat fluxes (10,000 to 80,000 W/m²), all the shrouds resulted in a considerable enhancement in the boiling performance. The 60° × 8.5° shroud appears to be the best selection for all practical heat fluxes.

I. PERFORMANCE OF GEWA-T TUBE WITH WIRE WRAPS IN INTER-FIN GAP

A series of runs were made with two to five 0.1 mm-diameter, copper wire wraps in the inter-fin gap of tube 1. Figures 17, 18, 19 and 20 show data with wire wraps of 2, 3, 4 and 5, respectively. It can be seen that all of these curves show increases in boiling performance at all wall superheats for decreasing heat flux values. This enhancement is most probably due to the increase in the nucleation sites within the inter-fin cavities. However, there is a small reduction in performance in the natural convection process probably owing to that wires could act as an insulating material due to the thermal contact resistance between the wires and the inter-fin area.

Table 2 also shows that the use of three wires resulted in the best performance increase. This combination resulted in a 341 percent improvement in the boiling heat-transfer

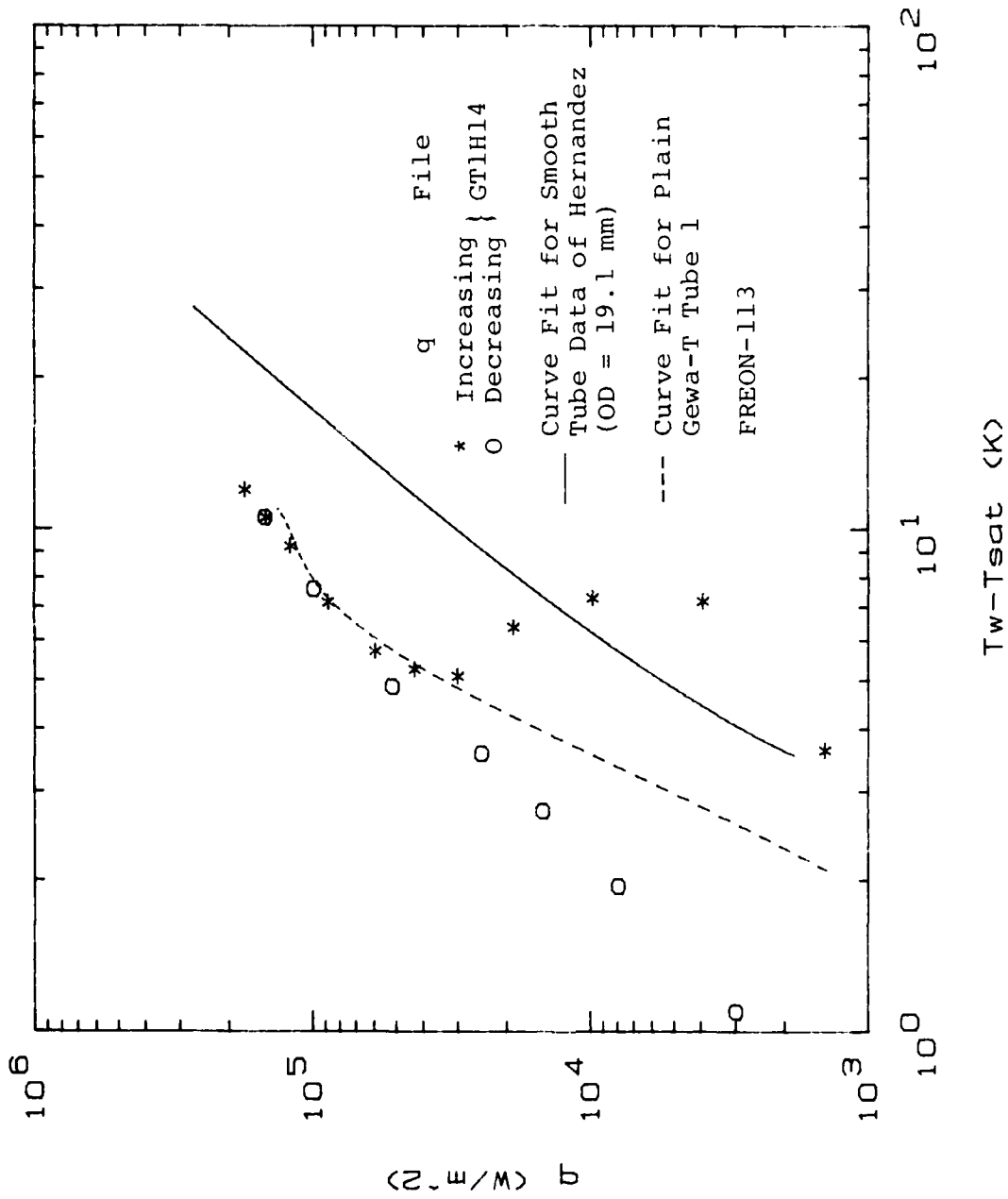


Figure 17. Effect of Two Wires Wrapped in the Inter-fin Cavity of Tube 1 on Boiling Performance

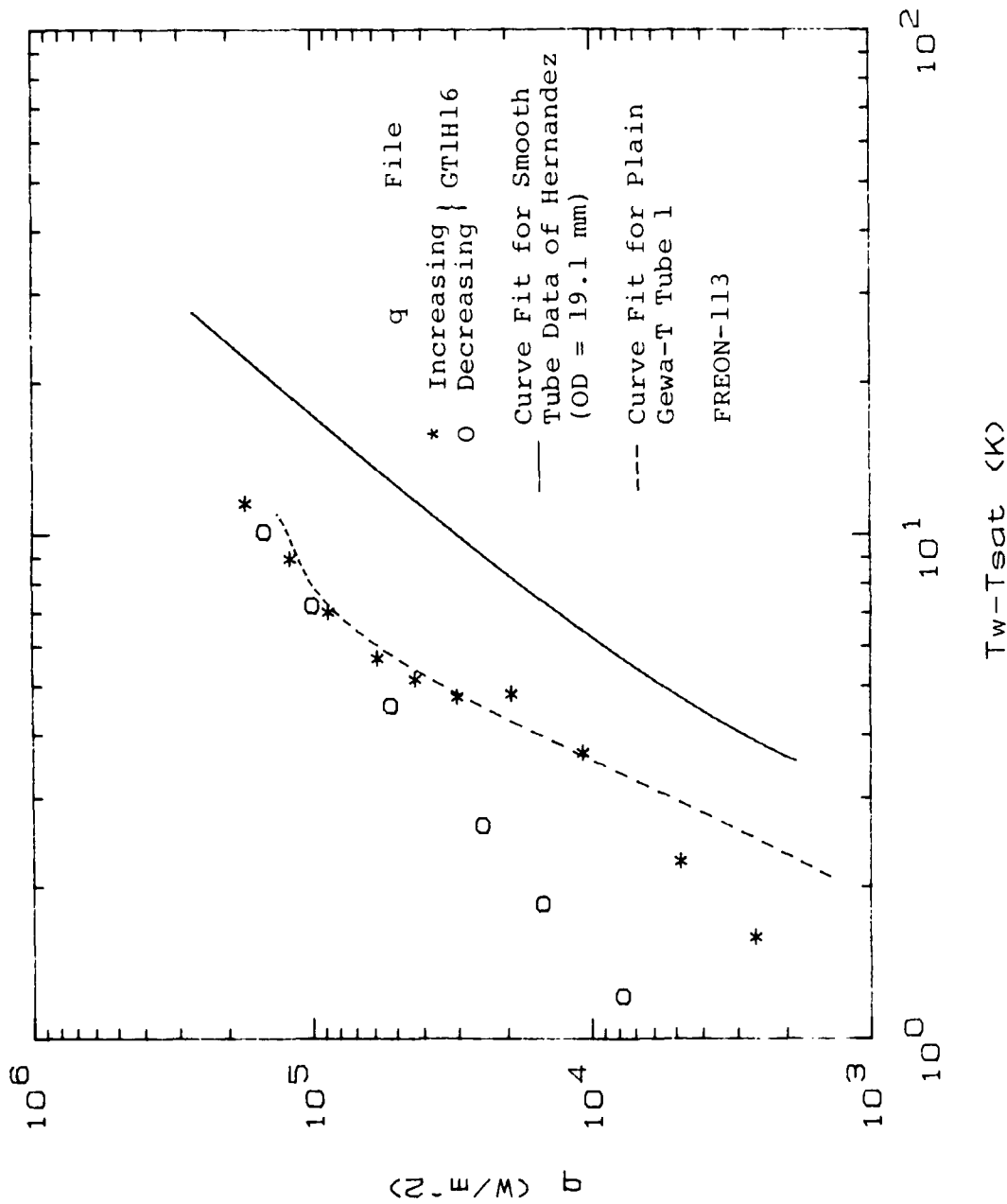


Figure 18. Effect of Three Wires Wrapped in the Inter-fin Cavity of Tube 1 on Boiling Performance

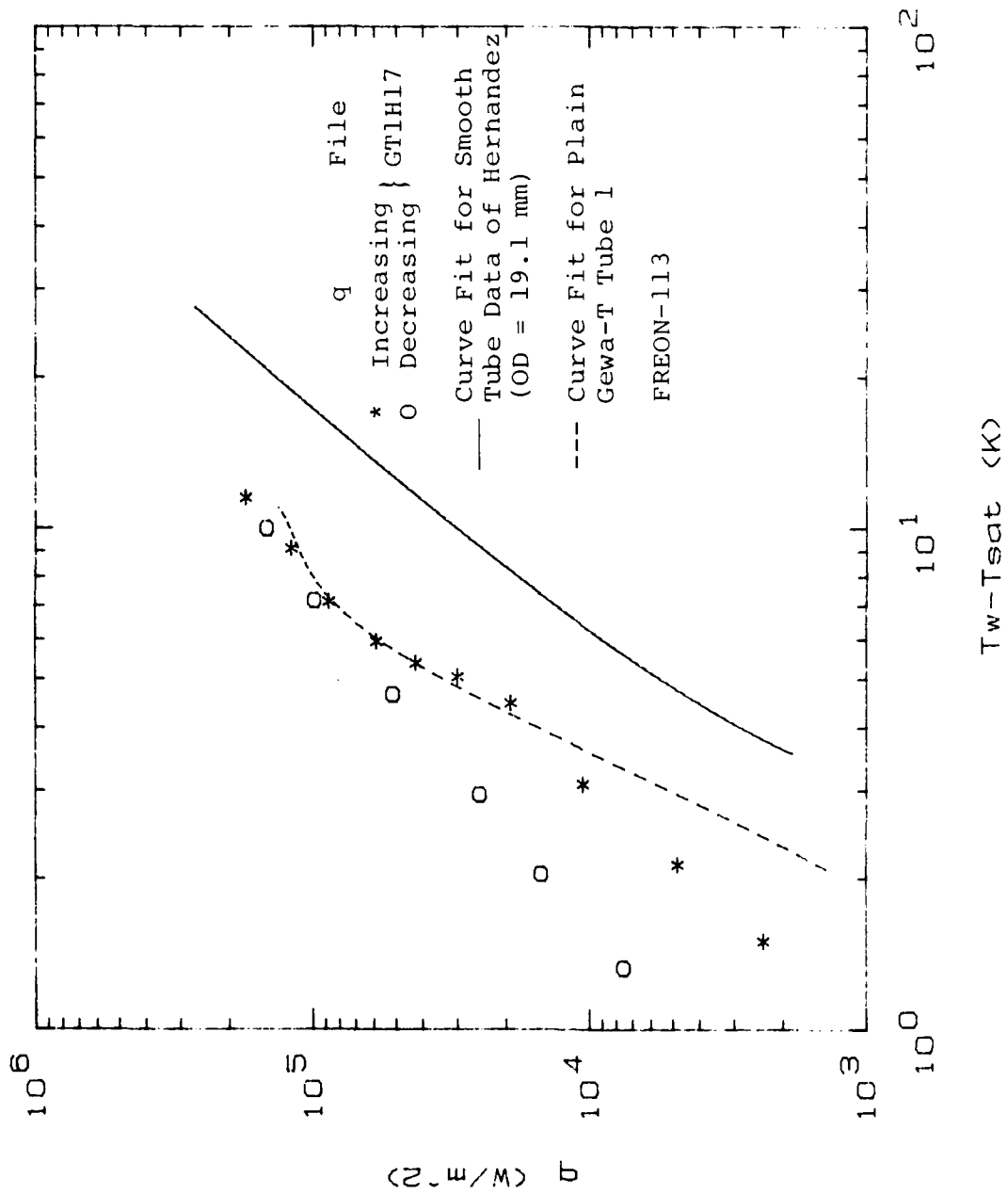
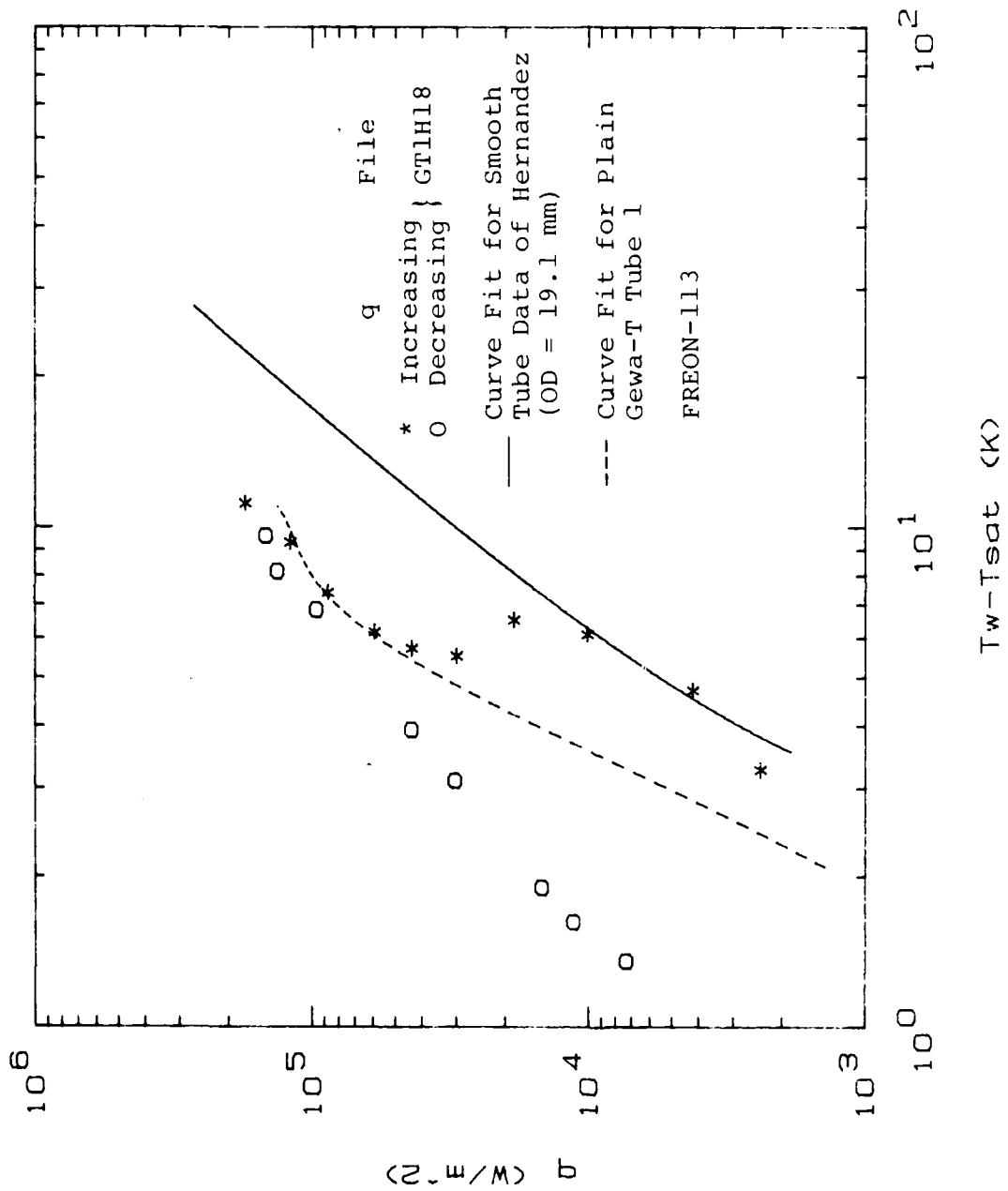


Figure 19. Effect of Four Wires Wrapped in the Inter-fin Cavity of Tube 1 on Boiling Performance



coefficient over the smooth tube value at a wall superheat of 1.4 K.

J. BOILING PERFORMANCE OF TUBE 1 WITH $60^\circ \times 8.5^\circ$ SHROUD AND THREE WIRES

Data were also taken to combine the best shroud and the best number of wire wraps in the inter-fin channel. For this purpose, three wire wraps were added to the inter-fin channel and data were taken with the $60^\circ \times 8.5^\circ$ shroud. As Figure 21 and Table 2 show, this combination resulted in a performance yet superior to the use of three wires or the use of $60^\circ \times 8.5^\circ$ shroud separately. Table 2 shows that this arrangement resulted in 481 percent increase in the boiling heat-transfer coefficient over the smooth-tube value at a heat flux of $10,000 \text{ W/m}^2$.

K. EFFECTS OF FIN-TIP GAP AND FIN DENSITY OF GEWA-T TUBES ON BOILING PERFORMANCE

As described earlier, six Gewa-T surfaces were tested during this stage of the investigation; tubes 2, 3, and 4 had a fin density of 0.75 fins/mm, and tubes 5, 6 and 7 with a fin density of 1.02 fins/mm, and each set of tubes with fin-tip gaps of 0.15, 0.25 and 0.33 (see Table 1).

Micrographs were obtained for all enhanced surfaces on a Scanning Electron Microscope with a magnification of 50X. Figure 5 shows micrographs representing tubes 2 and 5. Computed surface areas and area ratios (with respect to smooth tube) are listed in Table 3.

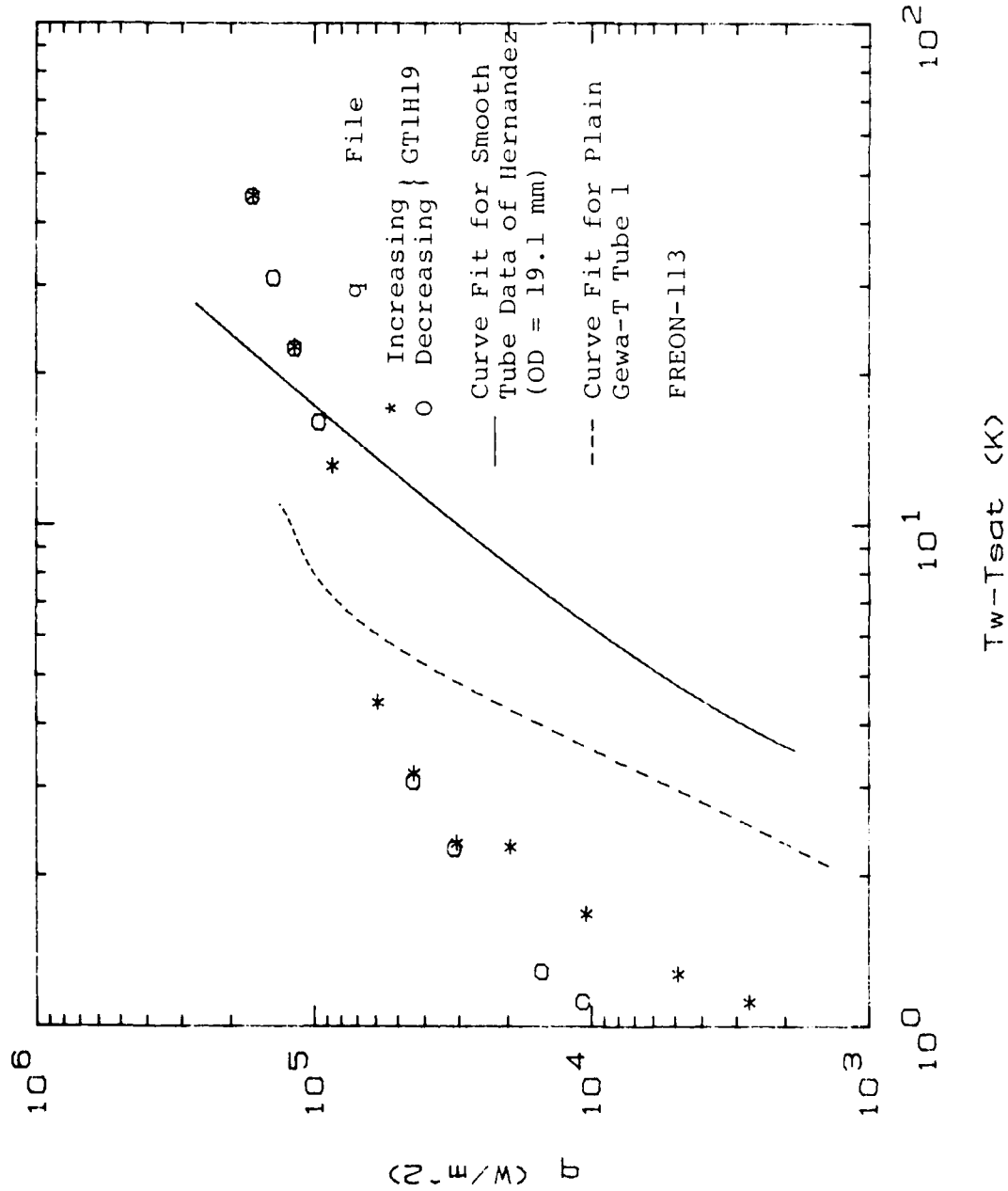


Figure 21. Effect of Three Wires Wrapped in the Inter-fin Cavity with 60° · 8.5° Shroud on Gewa-T Tube 1 on Boiling Performance

TABLE 3

Computed Surface Areas and Area Ratios

Tube	Cavity and Fin ₂ Surface Area (m ²)	Total Surface Area (m ²)	A _F /A _{SMOOTH}
1	240.47 × 10 ⁻⁶	8.818 × 10 ⁻³	---
2	288.01 × 10 ⁻⁶	10.944 × 10 ⁻³	2.74
3	305.34 × 10 ⁻⁶	11.603 × 10 ⁻³	2.91
4	285.07 × 10 ⁻⁶	10.833 × 10 ⁻³	2.72
5	256.04 × 10 ⁻⁶	13.314 × 10 ⁻³	3.60
6	248.61 × 10 ⁻⁶	12.928 × 10 ⁻³	3.50
7	267.91 × 10 ⁻⁶	13.931 × 10 ⁻³	3.77

It can be seen that tubes with a higher fin density (1.02 fins/mm) result in larger area ratios than the tubes with lower fin density (0.75 fins/mm). However, for a given fin density, the variation of the area ratio with fin-tip gap is not conclusive.

Figures 22 through 27 show data taken on tubes 2 through 7, respectively. These results are also listed in Table 2. This table shows that tube 6 (with a fin density of 1.02 fins/mm and a fin-tip gap of 0.25 mm) resulted in the highest heat flux at all values of wall superheat.

To investigate the effects of fin density and fin-tip gap on boiling heat-transfer performance, the results presented in Figures 22 through 27 (which showed variations of

APPENDIX A

DATA REDUCTION PROGRAM

```

1000 FILE NAME: DRPC
1010 DATE: May 16, 1984
1020 REVISED: July 20, 1984
1030
1040 BEEP
1050 PRINTER IS
1060 PRINT USING "4X, ""Select option: """"
1070 PRINT USING "5X, ""Taking data or re-processing previous data""""
1080 PRINT USING "6X, ""Plotting data""""
1090 INPUT Idp
1100 IF Idp=0 THEN CALL Main
1110 IF Idp=1 THEN CALL Plot
1120 END
1130 SUB Main
1140 COM /C= C(7)
1150 DIM Emf(9), T(9)
1160 DATA 0.10086091, 25727.94369, -757345.8295, 78025595.81
1170 DATA -9247486589.6, 97688E+11, -2.66192E+13, 3.94078E+14
1180 READ C(*)
1190 BEEP
1200 INPUT "SELECT TUBE OD (0=0.75 in. 1=1.0 in)".Itd
1210 IF Itd=0 THEN
1220 D1=.0159 ! Diameter at thermocouple positions
1230 D2=.0193 ! Diameter of test section to the base of fins
1240 D1=.0193 ! Inside diameter of unenhanced ends
1250 D0=.0190 ! Outside diameter of unenhanced ends
1250 L=.0490 ! Length of enhanced surface
1270 Lu=.0319 ! Length of unenhanced surface at the ends
1280 ELSE
1290 D1=.01796
1300 D2=.0231
1310 D1=.02032
1320 D0=.02222
1330 L=.0508
1340 Lu=.03175
1350 END IF
1360 Lc=Lu+(D0-D1)/2
1370 A=PI*(D02-D12)/4
1380 P=PI*D0
1390 Kcu=385 ! Thermal conductivity of Copper
1400 PRINTER IS
1410 CLEAR 709
1420 BEEP
1430 INPUT "ENTER MONTH, DATE AND TIME (MM:DD:HH:MM:SS)".Dates
1440 OUTPUT 709:"ID":Dates
1450 OUTPUT 709:"TD"
1460 ENTER 709:Dates
1470 PRINT " Month, date and time :":Dates
1480 PRINT
1490 PRINT USING "10X, ""NOTE: Program name : BOIL""""
1500 BEEP
1510 INPUT "ENTER DISK NUMBER".Dn
1520 PRINT USING "16X, ""Disk number = """, D7":Dn
1530 BEEP
1540 INPUT "ENTER INPUT MODE (0=0054A, 1=FILE)".Im
1550 Im=Im+1
1560 IF Im=1 THEN
1570 BEEP
1580 INPUT "GIVE A NAME FOR THE RAW DATA FILE".Dfiles
1590 PRINT USING "16X, ""New file name: """, D4A":Dfiles

```

VI. RECOMMENDATIONS

(1) Investigate the reason for the existence of a longitudinal temperature profile and take appropriate steps to alleviate this problem.

(2) Study the possibility of adding roughness in the inter-fin cavity of Gewa-T tubes. This operation should be performed before the rolling process to obtain the T-shaped fins.

(3) Repeat runs made during this investigation with water as the boiling medium.

This combination resulted in a 481 percent increase in boiling heat-transfer coefficient at a wall superheat of 1.1 K.

(6) The use of wires appears to be superior to the use of more expensive shrouds.

(7) Among the fin-tip gaps of 0.15, 0.25 and 0.35 mm tested, the 0.25 mm gap resulted in the best boiling performance.

(8) The Gewa-T tubes with a fin density of 1.02 fins/mm performed superior to a fin density of 0.75 fins/mm. At a wall superheat of 3.5 K, the lower-fin-density tube increased the boiling heat-transfer coefficient by 80 percent, while the higher-fin-density tube increased by 103 percent.

V. CONCLUSIONS

(1) Experimental observations revealed a non-uniform temperature distribution along test section. The bubble generation was seen to start at the two ends and migrate into the center as the heat flux was increased. No clear explanation is possible for this temperature distribution.

(2) Results of the present investigation showed very good repeatability with the results of Hernandez obtained under similar conditions.

(3) The use of shrouds improved the boiling heat-transfer coefficient of Gewa-T surface at all practical heat fluxes. However, a considerable reduction in heat-transfer coefficient was seen at very high heat fluxes ($> 100,000 \text{ W/m}^2$). Among the four shrouds tested, the shroud with $60^\circ \times 8.5^\circ$ openings resulted in the best performance verifying Hernandez's results. This shroud resulted in a 253 percent increase in boiling heat-transfer coefficient, over smooth tube, at a wall superheat of 1.8 K.

(4) The use of 0.1 mm-diameter wires (2 to 5) improved boiling heat-transfer coefficient at all practical heat fluxes. The use of 3 wires resulted in the best performance with a 341 percent increase in the heat-transfer coefficient (over the smooth-tube value) at a wall superheat of 1.4 K.

(5) Further improvement in boiling performance was obtained by using the $60^\circ \times 8.5^\circ$ shroud with three wire wraps.

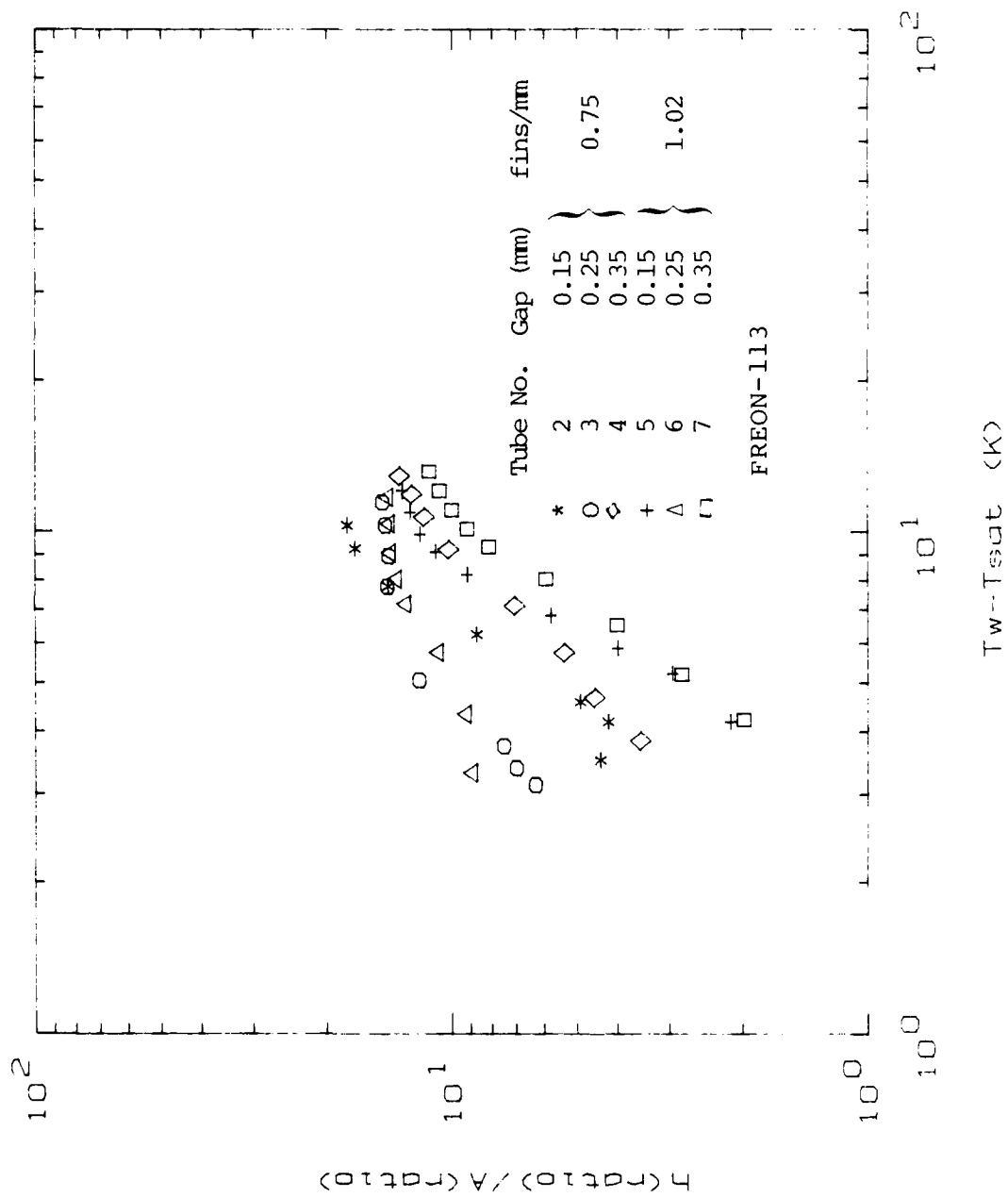


Figure 29. Enhancement Ratios of Gewa-T Tubes over Smooth Tube Based on Actual Area

explanations given above should be valid for the poorer performance of tubes 2 and 4.

It can be seen that all tubes show smaller enhancement ratios at low wall superheats, and the above-mentioned differences in performance are more pronounced. On the other hand, all the tubes show greater enhancements at larger wall superheats and they seem to approach a common enhancement ratio. The increase in enhancement is believed to be due to the increased chimney effect, which helps to remove vapor bubbles from channels resulting in a thinner liquid film at the hot boiling surface. When heat flux is further increased, vapor can provide a blanket around the hot surface, which may eventually result in a critical heat flux. It appears that the critical heat flux is not strongly dependent on the fin density or fin-tip gap.

The results shown in Figure 28 were also replotted as shown in Figure 29 to further study the performance of these six tubes. This figure shows the variation in enhancement ratio obtained beyond the area increase (i.e., the ratio of heat-transfer enhancement/area ratio) as a function of wall superheat. It is evident that obviously all tubes resulted in enhancement ratios beyond the area increase.

In summary, a fin density of 1.02 fins/mm resulted in performance superior to a fin density of 0.75 fins/mm. Also, in both cases, a fin-tip gap of 0.25 mm resulted in the best performance.

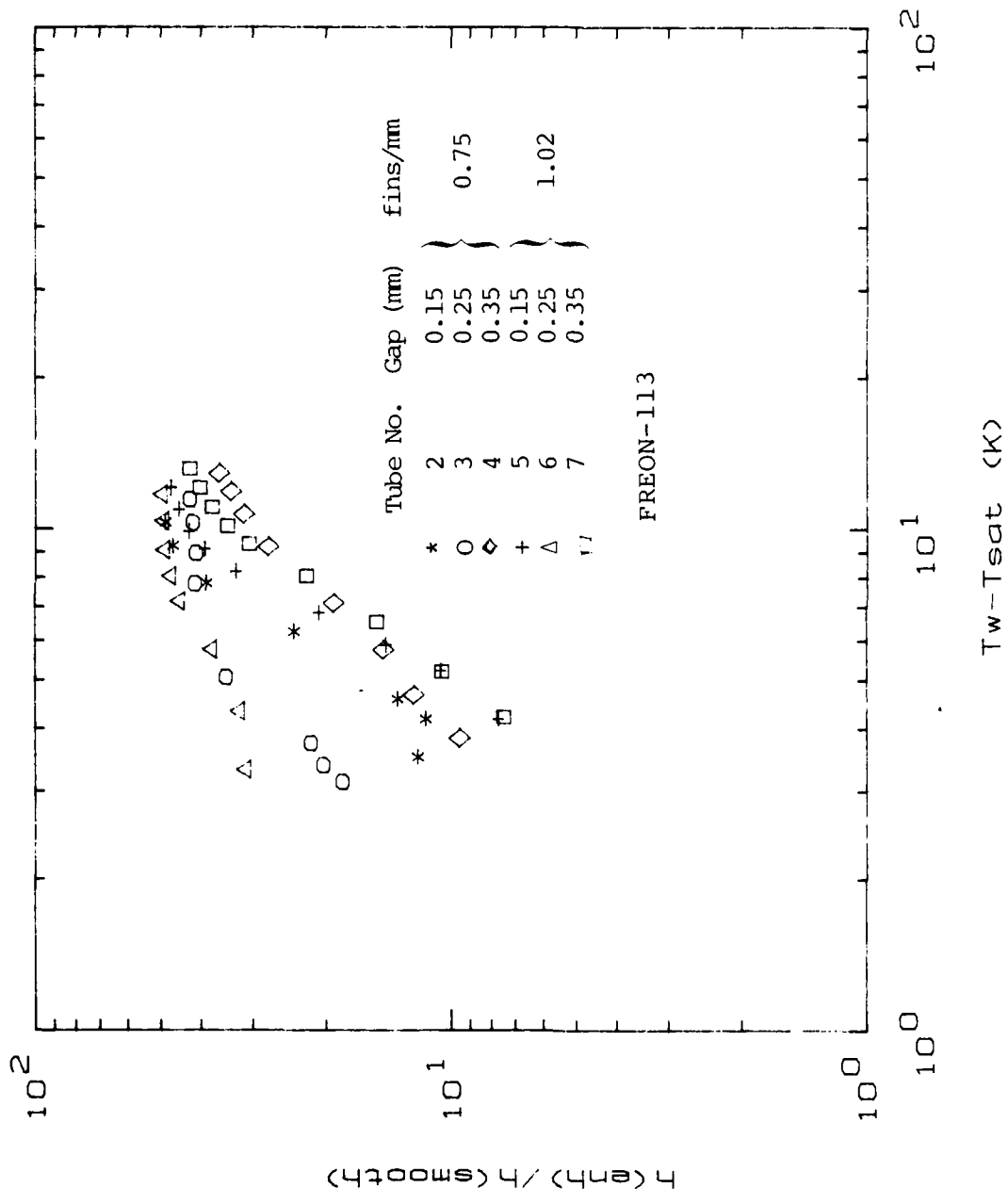


Figure 28. Enhancement Ratios of Gewa-T Tubes over Smooth Tubes Based on Nominal Area

heat flux as a function of wall superheat) were re-plotted on a different basis as shown in Figure 28. This figure shows the variations of the enhancement of heat-transfer coefficient, over the smooth-tube value, with wall superheat for all six tubes. It is evident that tube 6, which has a fin density of 1.02 fins/mm and a fin-tip gap of 0.25 mm results in the maximum enhancement at all wall superheat values.

Tube 5 shows poorer performance than tube 6. This poorer performance is believed to be due to the fact that the smaller fin-tip gap disrupts the flow of liquid into the channels and/or the vapor flow out of the channels. Tube 7 (which has the largest fin-tip gap of 0.35 mm) shows the poorest performance among the set of these tubes with a fin density of 1.02 fins/mm. As visually observed during experimental runs, this tube ejected a considerable portion of vapor bubbles radially along tube periphery. This premature departure of vapor bubbles results in a lower performance by producing a thicker liquid film at the hot surface.

In comparison with the results for tubes 5, 6 and 7, the curves representing tubes 2, 3 and 4 show that for a given fin-tip gap, the performance has decreased with decrease in fin density. This observation is believed to be due to the presence of a greater number of channels (for a given length of tube) in the higher-fin-density tubes. Again, for a fin density of 0.75 fins/mm, the 0.25 mm fin-tip gap (tube 3) resulted in the best boiling performance. The same

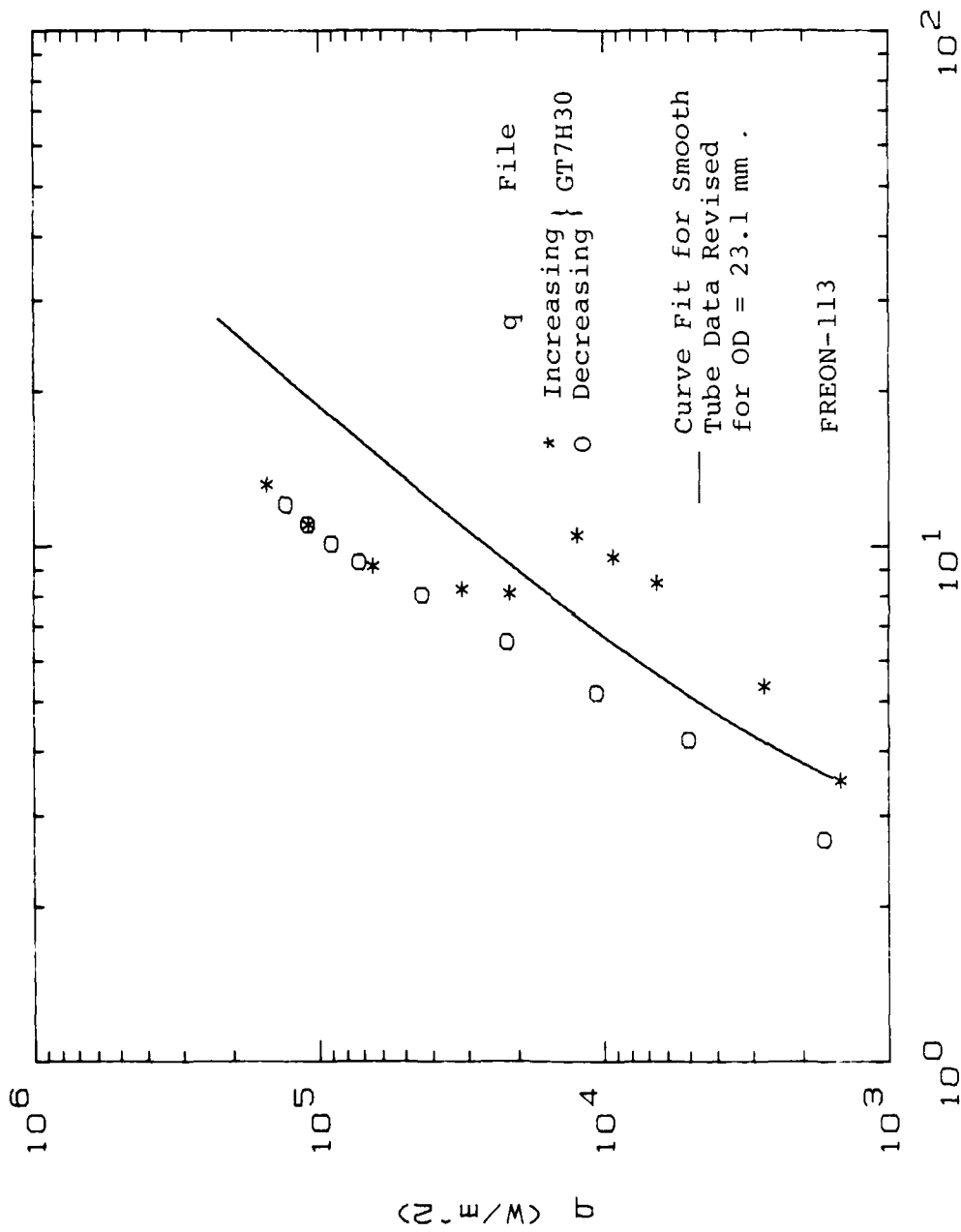


Figure 27. Boiling Performance of Gewa-T Tube 7
 $T_w - T_{\text{sat}}$ (K)

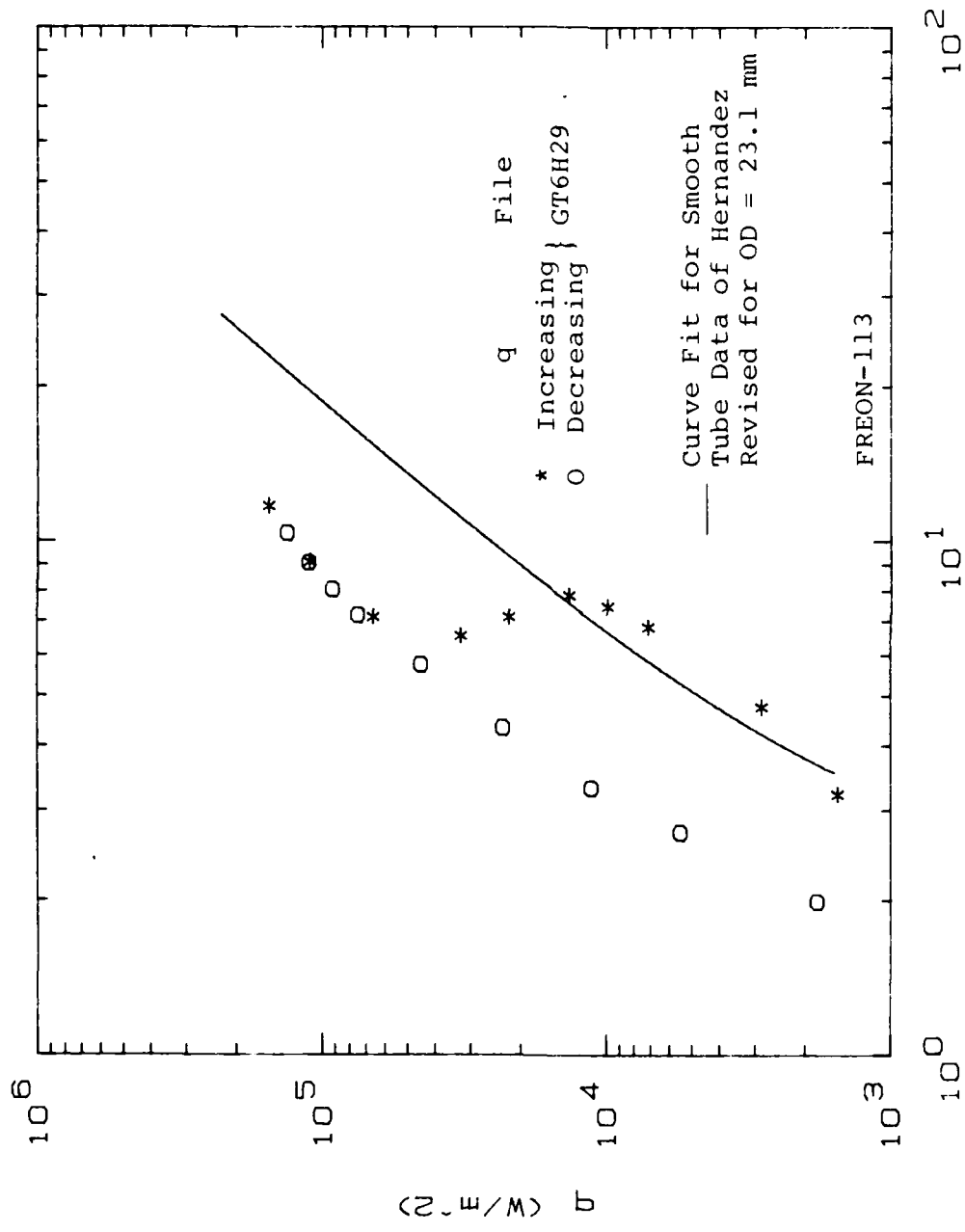


Figure 26. Boiling Performance of Gewa-T Tube 6

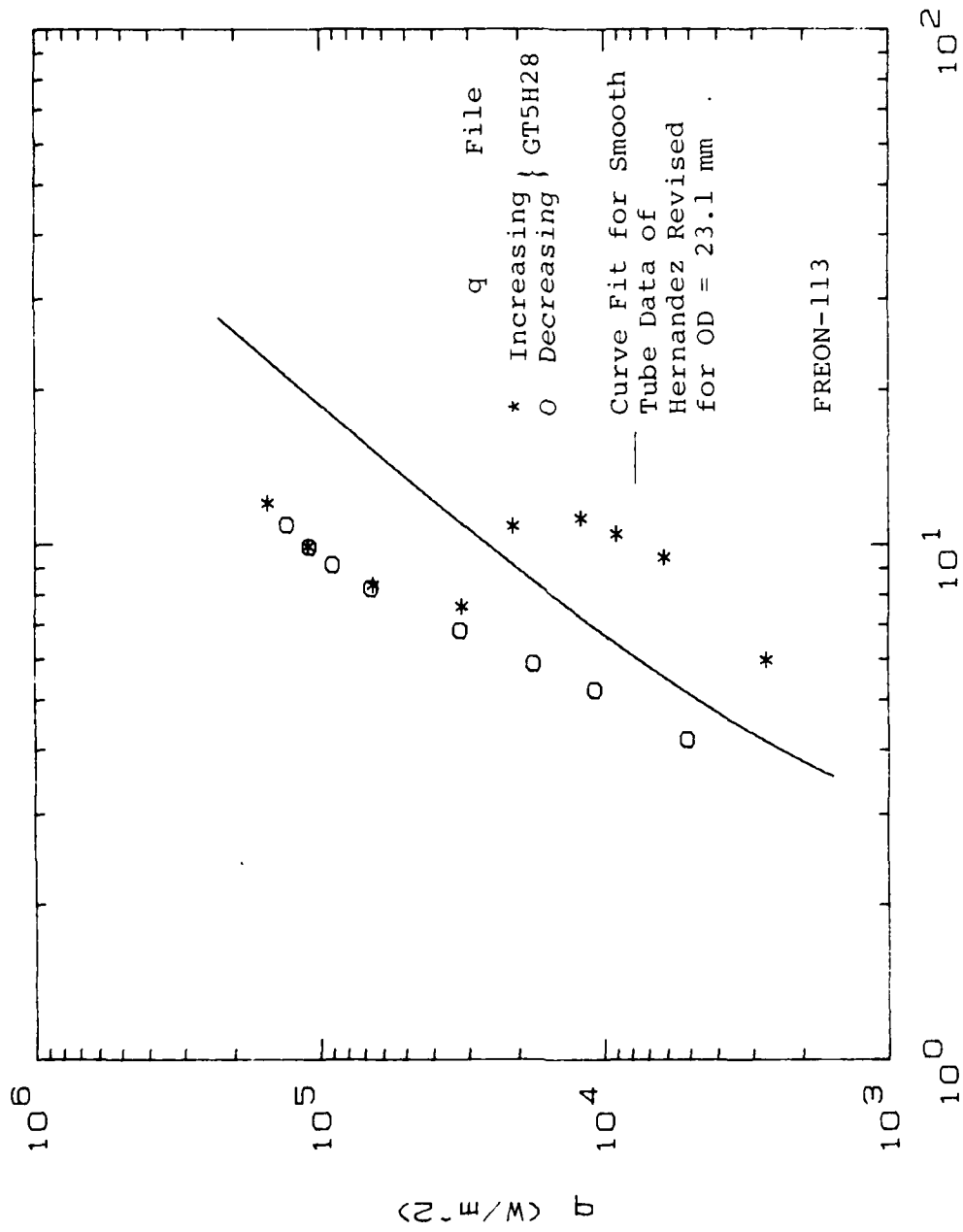


Figure 25. Boiling Performance of Gewa-T Tube 5

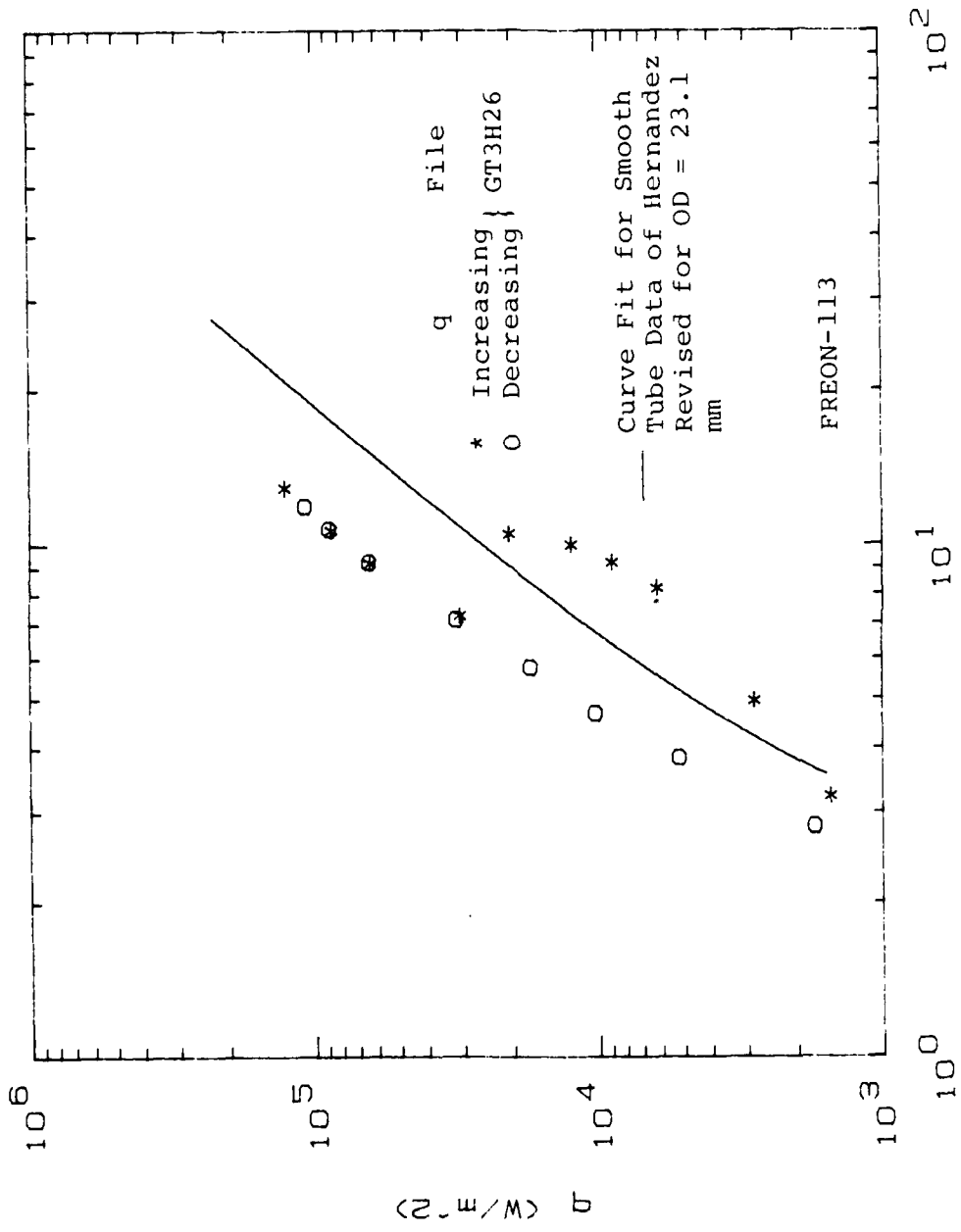


Figure 24. Boiling Performance of Gewa-T Tube 4

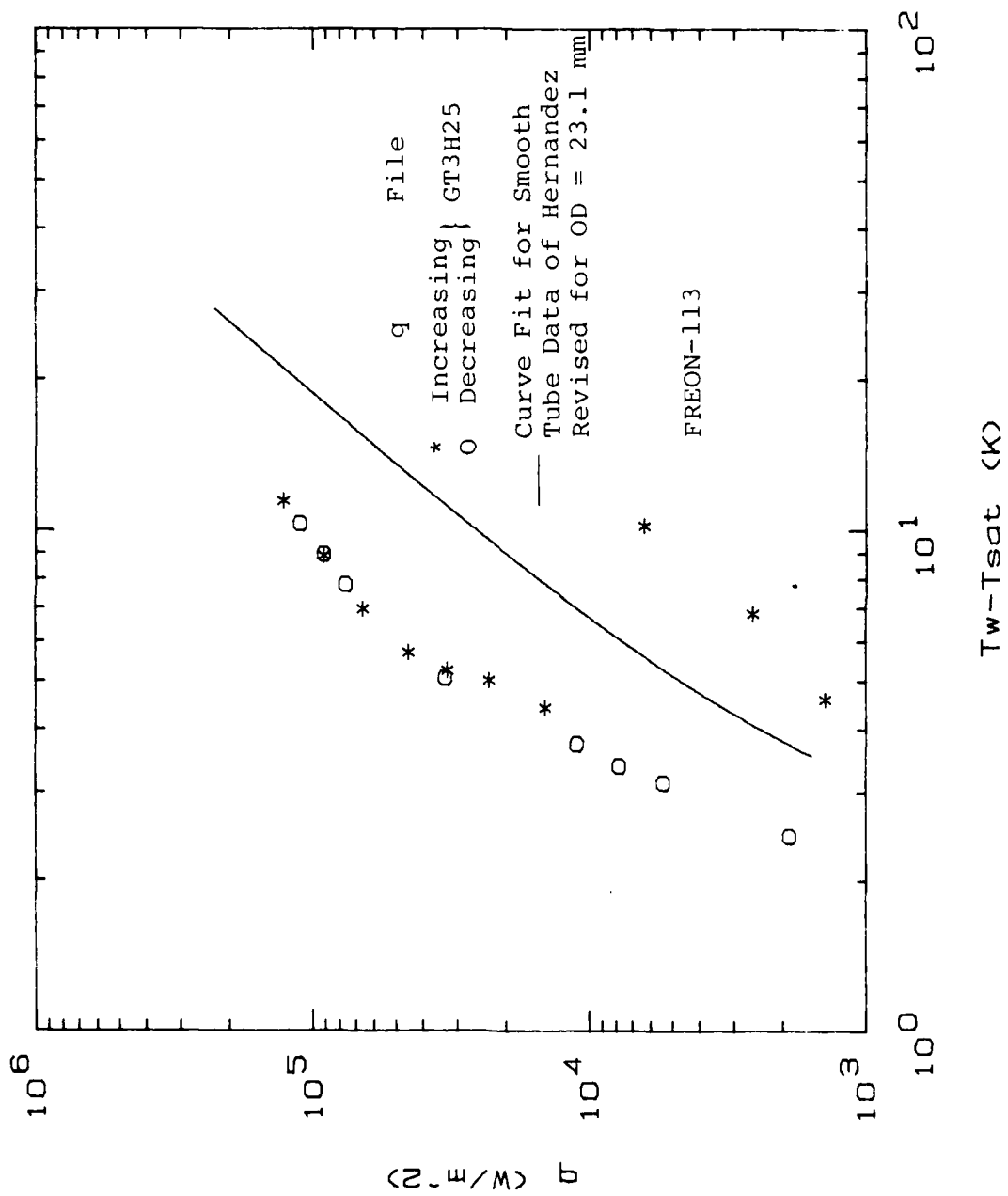


Figure 23. Boiling Performance of Gewa-T Tube 3

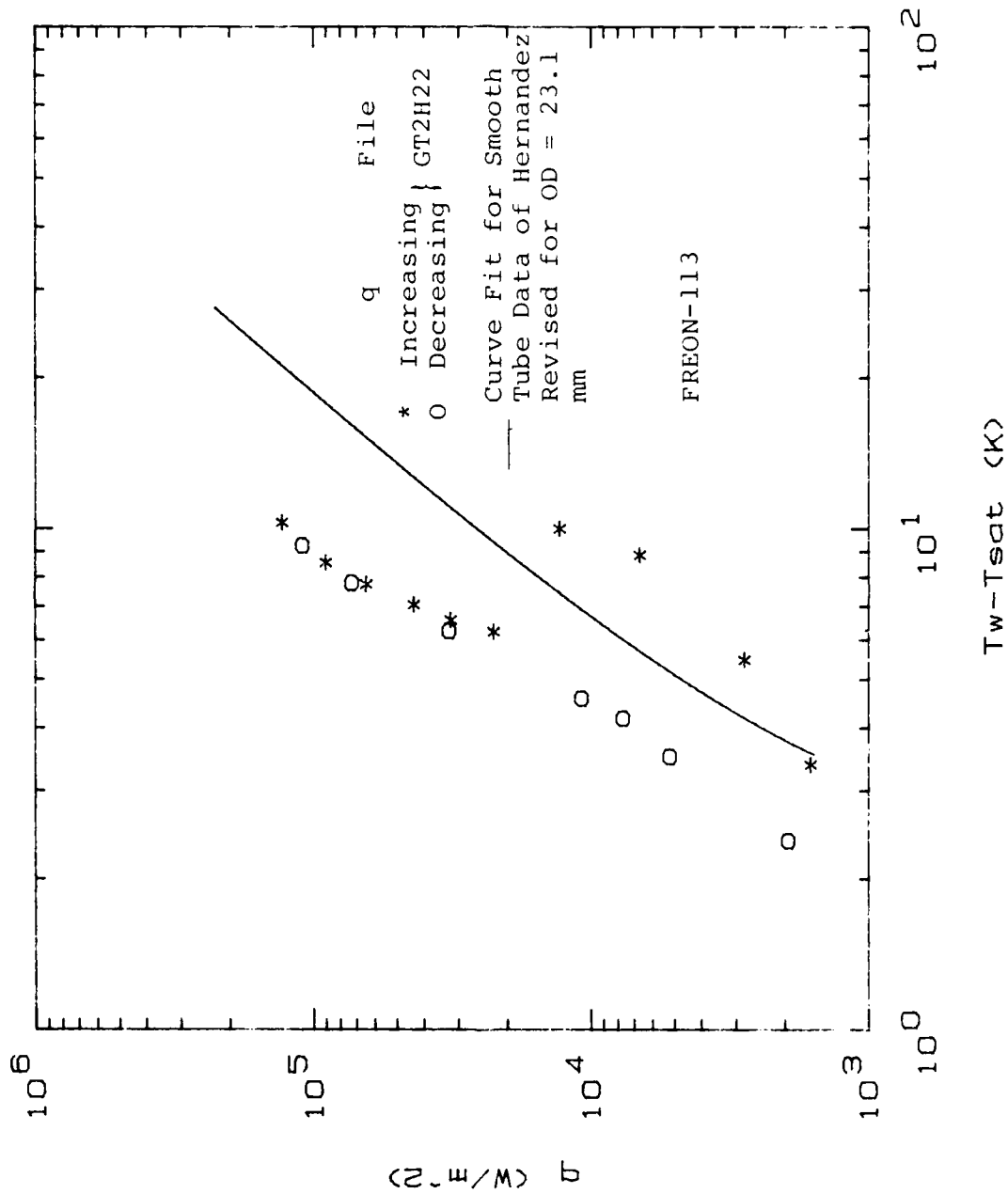


Figure 22. Boiling Performance of Gewa-T Tube 2

```

1500 BEEP
1510 INPUT "ENTER FLUID (0=FREON-113,1=WATER)".Cf
1620 Cf=Cf-1
1530 CREATE BDAT D_files.20
1640 ASSIGN @File TO D_files
1650 OUTPUT @File:Date$.Cf
1660 ELSE
1670 BEEP
1680 INPUT "GIVE THE NAME OF THE EXISTING DATA FILE".D_files
1690 BEEP
1700 Ihc=0
1710 INPUT "ENTER 1 IF USING FILE NUMBER < 25".Ihc
1720 PRINT USING "16X. ""Old file name: ""'.14A":D_files
1730 BEEP
1740 INPUT "ENTER THE NUMBER OF RUNS STORED".Nrun
1750 ASSIGN @File TO D_files
1760 ENTER @File:Dold$.Cf
1770 PRINT USING "16X. ""This output for file created at ""'.14A":Dold$
1780 END IF
1790 BEEP
1800 INPUT "GIVE A NAME FOR PLOT FILE".P_files
1810 CREATE BDAT P_files.5
1820 ASSIGN @Plot TO P_files
1830 IF Cf=1 THEN PRINT USING "16X. ""Fluid : Freon-113""
1840 IF Cf=2 THEN PRINT USING "16X. ""Fluid : Water""
1850 BEEP
1860 INPUT "ENTER OUTPUT VERSION (1=SHORT,0=LONG)".Iov
1870 IF Iov=0 THEN Iov=2
1880 BEEP
1890 INPUT "ENTER NUMBER OF DEFECTIVE TCS (0=DEFAULT)".Idtc
1900 IF Idtc>0 THEN
1910 BEEP
1920 IF Idtc=1 THEN
1930 INPUT "ENTER DEFECTIVE TC LOCATION".Ldtc1
1940 PRINT USING "16X. ""TC is defective at location ""'.D":Ldtc1
1950 END IF
1960 IF Idtc=2 THEN
1970 INPUT "ENTER DEFECTIVE TC LOCATIONS".Ldtc1.Ldtc2
1980 PRINT USING "16X. ""TC are defective at locations ""'.D,4X,D":Ldtc1.Ldtc2
1990 END IF
2000 END IF
2010 IF Im=1 THEN
2020 BEEP
2030 INPUT "ENTER BAROMETRIC PRESSURE (inHg)".Patm
2040 Patm=Patm+2*1500/13500
2050 OUTPUT @File:Patm
2060 ELSE
2070 ENTER @File:Patm
2080 IF Ihc=1 THEN Patm=Patm+2*1500/13500
2090 END IF
2100 Patm=Patm*25.4*14.696/760
2110 Tsat=FNIsat(Cf,Patm)
2120 PRINT USING "16X. ""Saturation temperature = ""'.3D,DD. "" (Deg C)""":Tsat
2130 J=1
2140 Sx=0
2150 Sy=0
2160 Sxs=0
2170 Sxy=0
2180 BEEP
2190 INPUT "HIT CONTINUE WHEN READY".Ok

```

```

2200 Repeat:
2210 IF In=1 THEN
2220 OUTPUT 709:"AR AF29 AL38 VRS"
2230 FOR I=0 TO 3
2240 OUTPUT 709:"AS SA"
2250 Sum=0
2260 FOR J1=1 TO 20
2270 ENTER 709:E
2280 Sum=Sum+E
2290 NEXT J1
2300 Emf(I)=Sum/20
2310 NEXT I
2320 BEEP
2330 INPUT "ENTER HEATER VOLTAGE, Vh (V)".Vh
2340 BEEP
2350 INPUT "ENTER RESISTOR VOLTAGE, Vr (V)".Vr
2360 ELSE
2370 ENTER @File:Emf(*),Vr,Vh
2380 END IF
2390 Twa=0
2400 FOR I=0 TO 9
2410 IF Idtc>0 THEN
2420 IF (I+1)=Ldte1 OR (I+1)=Ldte2 THEN
2430 T(I)=99.99
2440 GOTO 2490
2450 END IF
2460 END IF
2470 T(I)=FNTvsv(Emf(I))
2480 IF I<8 THEN Twa=Twa+T(I)
2490 NEXT I
2500 Twa=Twa/(8-Idtc)
2510 Tld=T(9)
2520 Tv=T(8)
2530 Rho=FNRho(Cf,Tsat)
2540 Mu=FNMu(Cf,Tsat)
2550 K=FNK(Cf,Tsat)
2560 Cp=FNCo(Cf,Tsat)
2570 Beta=FNBeta(Cf,Tsat)
2580 Ni=Mu/Rho
2590 Alpha=K/(Rho*Cp)
2600 Pr=Ni/Alpha
2610 Amp=Vr/2.031
2620 Q=Vh*Amp
2630 Tw=Twa-Q*LOG(D2/D1)/(2*PI*Kcu*L)
2640 Thetab=Tw-Tsat
2650 IF Thetab<0 THEN
2660 BEEP
2670 DISP "WALL<TSAT (HIT CONTINUE WHEN READY)"
2680 PAUSE
2690 GOTO 2210
2700 END IF
2710 Hbar=190
2720 Fe=(Hbar+P/(Kcu*A))*.5*Lo
2730 Tann=FNtanh(Fe)
2740 Theta=Thetab*Tann/Fe
2750 Xx=(9.31+Beta*Thetab*Do/3*Tann/(Fe*Ni*Alpha)).16667
2760 Yy=(1+(.559/Pr))^(9/15)^(8/27)
2770 Hbarc=K/Do*(.6+.387*Yy/Xx)^.2
2780 IF ABS((Hbar-Hbarc)/Hbarc)>.001 THEN
2790 Hbar=(Hbar+Hbarc)*.5
2800 GOTO 2720

```

```

2810 END IF
2820 Q1=(Hbar*P*cu+A) .5*Thetab*Tann
2830 Qc=Q-2*Q1
2840 As=PI*Q2-L
2850 Qdp=Qc/As
2860 IF Iov=1 THEN PRINT USING "10X,0D,2X,3D,0D,2X,2(Z,4DE,2X),0D,0D":J,Twa,Hba
r,Qdp,Thetab
2870 IF Iov=2 THEN
2880 PRINT USING "10X, ""Data set number = "" ,0D":J
2890 PRINT USING "10X, ""Position number : " 1 2 3 4 5 6
7
3 """:J,I,T(1),T(2),T(3),T
(4),T(5),T(6),T(7)
2910 PRINT USING "10X, ""Tltd Tvapr Twa Hbar Qdp Thetab """:
Tld,Tv,Twa,Hbar,Qdp,Thetab
2920 PRINT USING "9X,3(3D,DD,2X),2(Z,4DE,2X),2D,DD":Tld,Tv,Twa,Hbar,Qdp,Thetab
2930 END IF
2940 IF Im=1 THEN
2950 BEEP
2960 INPUT "OK TO STORE THIS DATA SET (I=Y,0=N)?:",Ok
2970 END IF
2980 IF Ok=1 OR Im=2 THEN J=J+1
2990 IF Ok=1 AND Im=1 THEN OUTPUT @File:Emf(*),Vr,Vh
3000 IF Im=2 OR Ok=1 THEN OUTPUT @Plot:Qdp,Thetab
3010 IF Im=1 THEN
3020 BEEP
3030 INPUT "WILL THERE BE ANOTHER RUN (I=Y,0=N)?:",Go_on
3040 Nrun=J
3050 IF Go_on<>1 THEN 3110
3060 WAIT 300
3070 IF Go_on=1 THEN Repeat
3080 ELSE
3090 IF J<Nrun+1 THEN Repeat
3100 END IF
3110 IF Im=1 THEN
3120 BEEP
3130 PRINT
3140 PRINT USING "10X, ""NOTE: "" ,ZZ, "" data runs were stored in file "" ,10A":J-
1,0_files
3150 END IF
3160 BEEP
3170 PRINT
3180 PRINT USING "10X, ""NOTE: "" ,ZZ, "" X-Y pairs were stored in plot data file
"" ,10A":J-1,0_files
3190 ASSIGN @File TO *
3200 ASSIGN @Plot TO *
3210 BEEP
3220 INPUT "LIKE TO PLOT DATA (I=Y,0=N)?:",Ok
3230 IF Ok=1 THEN
3240 CALL Plot
3250 END IF
3260 SUBEND
3270 DEF FNMu(Cf,T)
3280 IF Cf=1 THEN
3290 RANGE: 20 TO 50 DEG C
3300 Mu=8.9629819E-4-T*(1.1094609E-5-T*5.5668229E-8)
3310 END IF
3320 IF Cf=2 THEN
3330 A=247.3/(7+103.15)
3340 Mu=2.4E-5+10 A
3350 END IF

```

```

3360 RETURN Mu
3370 FNEND
3380 DEF FNCp(Cf,T)
3390 IF Cf=1 THEN
3400! RANGE: 0 TO 30 DEG C
3410 Cp=9.2507273E-1+T*(9.3400433E-4+1.7207792E-5*T)
3420 END IF
3430 IF Cf=2 THEN
3440 Cp=4.21120858-T*(2.26826E-3-T*(4.42361E-5+2.71428E-7*T))
3450 END IF
3460 RETURN Cp*1000
3470 FNEND
3480 DEF FNRho(Cf,T)
3490 IF Cf=1 THEN
3500! RANGE: 30 TO 80 DEG C
3510 Ro=1.6207479E+3-T*(2.2186346+T*2.3578291E-3)
3520 END IF
3530 IF Cf=2 THEN
3540 Ro=999.52946+T*(.01269-T*(5.482513E-3-T*1.234147E-5))
3550 END IF
3560 RETURN Ro
3570 FNEND
3580 DEF FNPp(Cf,T)
3590 Pp=FNCp(Cf,T)*FNMu(Cf,T)/FNK(Cf,T)
3600 RETURN Pp
3610 FNEND
3620 DEF FNK(Cf,T)
3630 IF Cf=1 THEN
3640! RANGE: 30 TO 90 DEG C
3650 K=8.2095238E-2-T*(2.2214286E-4+T*2.3809524E-8)
3660 END IF
3670 IF Cf=2 THEN
3680 X=(T+273.15)/273.15
3690 K=-.92247+X*(2.8395-X*(1.8007-X*(.52577-.07344*X)))
3700 END IF
3710 RETURN K
3720 FNEND
3730 DEF FNTanh(X)
3740 P=EXP(X)
3750 Q=EXP(-X)
3760 Tanh=(P-Q)/(P+Q)
3770 RETURN Tanh
3780 FNEND
3790 DEF FNTvsV(V)
3800 CDM /Cc/ C(7)
3810 T=C(0)
3820 FOR I=1 TO 7
3830 T=T+C(I)*V*I
3840 NEXT I
3850 T=T+8.34643E-1-T*(2.4547896E-2-T*1.3722580E-4)
3860 RETURN T
3870 FNEND
3880 DEF FNBeta(Cf,T)
3890 Rop=FNRho(Cf,T+.1)
3900 Rom=FNRho(Cf,T-.1)
3910 Beta=-2/(Rop+Rom)*(Rop-Rom)/.2
3920 RETURN Beta
3930 FNEND
3940 DEF FNTsat(Cf,P)
3950 T1=10
3960 Th=10

```

```

3970 Ta=(Tl+Th)*.5
3980 Pc=FNPsat(Cf,Ta)
3990 IF ABS((P-Pc)/P)>.0001 THEN
4000 IF Pc>P THEN Th=Ta
4010 IF Pc<P THEN Tl=Ta
4020 GOTO 3970
4030 END IF
4040 RETURN Ta
4050 FNEND
4060 DEF FNPsat(Cf,Tc)
4061 IF Cf=1 THEN
4070 T=Tc*.18+32+459.6
4080 P=10*(33.0655-4330.98/T-9.2635*LGT(T)+2.0539E-3*T)
4081 END IF
4082 IF Cf=2 THEN
4083 P=Pvstw(Tc)
4085 END IF
4090 RETURN P
4100 FNEND
4110 SUB Plot
4120 DIM C(9)
4130 INTEGER I1
4140 PRINTER IS I
4150 Idv=1
4160 BEEP
4170 INPUT "LIKE DEFAULT VALUES FOR PLOT (Y=0=N)?" Idv
4180 BEEP
4190 PRINT USING "4X," "Select Option:"
4200 PRINT USING "4X," "0 a versus delta-T"
4210 PRINT USING "4X," "1 h versus delta-T"
4220 PRINT USING "4X," "2 h versus a"
4230 PRINT USING "4X," "3 h-ratio versus delta-T"
4240 INPUT Dpo
4250 IF Dpo=3 THEN
4260 BEEP
4270 INPUT "SELECT TUBE DIAMETER (0=.75,1=1.0 IN)".ItD
4280 END IF
4290 PRINTER IS 705
4300 IF Idv<>1 THEN
4310 BEEP
4320 INPUT "ENTER NUMBER OF CYCLES FOR X-AXIS".Cx
4330 BEEP
4340 INPUT "ENTER NUMBER OF CYCLES FOR Y-AXIS".Cy
4350 BEEP
4360 INPUT "ENTER MIN X-VALUE (MULTIPLE OF 10)".Xmin
4370 BEEP
4380 INPUT "ENTER MIN Y-VALUE (MULTIPLE OF 10)".Ymin
4390 ELSE
4400 Cy=3
4410 IF Dpo=0 THEN
4420 Cx=2
4430 Xmin=1
4440 Ymin=1000
4450 END IF
4460 IF Dpo=1 THEN
4470 Cx=3
4480 Xmin=1
4490 Ymin=100
4500 END IF
4510 IF Dpo=2 THEN
4520 Cx=3

```

```

4530 Xmin=1000
4540 Ymin=1000
4550 END IF
4560 IF Dpo=3 THEN
4570 Cx=2
4580 Cy=3
4590 Xmin=1
4600 Ymin=1
4610 END IF
4620 END IF
4630 BEEP
4640 PRINT "IN:SP1:IP 2300,1800,8300,6800:"
4650 PRINT "SC 0,100,0,100:TL 2,0:"
4660 Sfx=100/Cx
4670 Sfy=100/Cy
4680 PRINT "PU 0,0 PD"
4690 Nn=9
4700 FOR I=1 TO Cx+1
4710 Xat=Xmin*10^(I-1)
4720 IF I=Cx+1 THEN Nn=1
4730 FOR J=1 TO Nn
4740 IF J=1 THEN PRINT "TL 2 0"
4750 IF J=2 THEN PRINT "TL 1 0"
4760 Xa=Xat*J
4770 X=LGT(Xa/Xmin)*Sfx
4780 PRINT "PA":X,".J: XT:"
4790 NEXT J
4800 NEXT I
4810 PRINT "PA 100,0:PU:"
4820 PRINT "PU PA 0,0 PD"
4830 Nn=9
4840 FOR I=1 TO Cy+1
4850 Yat=Ymin*10^(I-1)
4860 IF I=Cy+1 THEN Nn=1
4870 FOR J=1 TO Nn
4880 IF J=1 THEN PRINT "TL 2 0"
4890 IF J=2 THEN PRINT "TL 1 0"
4900 Ya=Yat*J
4910 Y=LGT(Ya/Ymin)*Sfy
4920 PRINT "PA 0,":Y,"YT"
4930 NEXT J
4940 NEXT I
4950 PRINT "PA 0,100 TL 0 2"
4960 Nn=9
4970 FOR I=1 TO Cx+1
4980 Xat=Xmin*10^(I-1)
4990 IF I=Cx+1 THEN Nn=1
5000 FOR J=1 TO Nn
5010 IF J=1 THEN PRINT "TL 0 2"
5020 IF J>1 THEN PRINT "TL 0 "
5030 Xa=Xat*J
5040 X=LGT(Xa/Xmin)*Sfx
5050 PRINT "PA":X,".100: XT"
5060 NEXT J
5070 NEXT I
5080 PRINT "PA 100,100 PU PA 100,0 PD"
5090 Nn=9
5100 FOR I=1 TO Cy+1
5110 Yat=Ymin*10^(I-1)
5120 IF I=Cy+1 THEN Nn=1
5130 FOR J=1 TO Nn

```

```

5140 IF J=1 THEN PRINT "TL 0 2"
5150 IF J>1 THEN PRINT "TL 0 1"
5160 Ya=Yat*J
5170 Y=LGT(Ya/Ymin)*Sfy
5180 PRINT "PD PA 100."Y,"YT"
5190 NEXT J
5200 NEXT I
5210 PRINT "PA 100.100 PU"
5220 PRINT "PA 0.-2 SR 1.5.2"
5230 Ii=LGT(Xmin)
5240 FOR I=1 TO Cx+1
5250 Xa=Xmin*10^(I-1)
5260 X=LGT(Xa/Xmin)*Sfx
5270 PRINT "PA":X,".0:"
5280 IF Ii>=0 THEN PRINT "CP -2,-2:LB10:PR -2.2:LB":Ii: ""
5290 IF Ii<0 THEN PRINT "CP -2,-2:LB10:PR 0.2:LB":Ii: ""
5300 Ii=Ii+1
5310 NEXT I
5320 PRINT "PU PA 0.0"
5330 Ii=LGT(Ymin)
5340 Y10=10
5350 FOR I=1 TO Cy+1
5360 Ya=Ymin*10^(I-1)
5370 Y=LGT(Ya/Ymin)*Sfy
5380 PRINT "PA 0.":Y,""
5390 PRINT "CP -4,-.25:LB10:PR -2.2:LB":Ii: ""
5400 Ii=Ii+1
5410 NEXT I
5420 IF Idv<>1 THEN
5430 BEEP
5440 INPUT "ENTER X-LABEL".Xlabel$
5450 BEEP
5460 INPUT "ENTER Y-LABEL".Ylabel$
5470 ELSE
5480 IF Dpo=0 THEN
5490 Xlabel$="Tw-Tsat (K)"
5500 Ylabel$="q (W/m 2)"
5510 END IF
5520 IF Dpo=1 THEN
5530 Xlabel$="Tw-Tsat (K)"
5540 Ylabel$="h (W/m 2.K)"
5550 END IF
5560 IF Dpo=2 THEN
5570 Xlabel$="a (W/m 2)"
5580 Ylabel$="h (W/m 2.K)"
5590 END IF
5600 IF Dpo=3 THEN
5610 Xlabel$="Tw-Tsat (K)"
5620 Ylabel$="h(enh)/h(smooth)"
5630 END IF
5640 END IF
5650 PRINT "SR 1 5.2:PU PA 50.-16 CP":-LEN(Xlabel$)/2:"0:LB":Xlabel$: ""
5660 PRINT "PA -14.50 CP 0.":-LEN(Ylabel$)/2*5/6:"DI 0.1:LB":Ylabel$: ""
5670 PRINT "CP 0.0 DI"
5680 Repeat:
5690 BEEP
5700 INPUT "WANT TO PLOT DATA FROM A FILE (Y=0=N)?".Ok
5710 IF Ok=1 THEN
5720 BEEP
5730 INPUT "ENTER THE NAME OF THE DATA FILE".D_files
5740 ASSIGN @File TO D_files

```

```

5750 BEEP
5760 BEEP
5770 INPUT "ENTER THE BEGINNING RUN NUMBER".Md
5780 BEEP
5790 INPUT "ENTER THE NUMBER OF X-Y PAIRS STORED".Npairs
5800 BEEP
5810 PRINTER IS 1
5820 PRINT USING "4X, ""Select a symbol: """"
5830 PRINT USING "4X, ""1 Star 2 Plus sign""""
5840 PRINT USING "4X, ""3 Circle 4 Square""""
5850 PRINT USING "4X, ""5 Rombus""""
5860 PRINT USING "4X, ""6 Right-side-up triangle""""
5870 PRINT USING "4X, ""7 Up-side-down triangle""""
5880 INPUT Sym
5890 PRINTER IS 705
5900 PRINT "PU DI"
5910 IF Sym=1 THEN PRINT "SM*"
5920 IF Sym=2 THEN PRINT "SM+"
5930 IF Sym=3 THEN PRINT "SMo"
5940 IF Md>1 THEN
5950 FOR I=1 TO (Md-1)
5960 ENTER @File:Ya,Xa
5970 NEXT I
5980 END IF
5990 FOR I=1 TO Npairs
6000 ENTER @File:Ya,Xa
6010 IF Opo=1 THEN Ya=Ya/Xa
6020 IF Opo=2 THEN
6030 Q=Ya
6040 Ya=Ya/Xa
6050 Xa=Q
6060 END IF
6070 IF Opo=3 THEN Ya=Ya/FNHsmooth(Xa,Itd)
6080 X=LGT(Xa/Xmin)*Sfx
6090 Y=LGT(Ya/Ymin)*Sfy
6100 IF Sym>3 THEN PRINT "SM"
6110 IF Sym<4 THEN PRINT "SR 1.4.2.4"
6120 PRINT "PA".X.Y, ""
6130 IF Sym>3 THEN PRINT "SR 1.2.1.6"
6140 IF Sym=4 THEN PRINT "UC2.4.99.0.-8.-4.0.0.8.4.0:"
6150 IF Sym=5 THEN PRINT "UC3.0.99.-3.-6.-3.6.3.6.3.-6:"
6160 IF Sym=6 THEN PRINT "UC0.5.3.99.3.-8.-5.0.3.8:"
6170 IF Sym=7 THEN PRINT "UC0.-5.3.99.-3.3.6.0.-3.-8:"
6180 NEXT I
6190 BEEP
6200 ASSIGN @File TO *
6210 GOTO 5690
6220 END IF
6230 PRINT "PU SM"
6240 BEEP
6250 INPUT "WANT TO PLOT A POLYNOMIAL (I=Y.0=N)?"Go_on
6260 IF Go_on=1 THEN
6270 BEEP
6280 INPUT "ENTER LOWER AND UPPER X-LIMITS".Xll,Xlu
6290 FOR Xx=0 TO Cx STEP Cx/200
6300 Xa=Xmin+10 Xx
6310 IF Xa<Xll OR Xa>Xlu THEN 6380
6320 Ya=FNpoly(Xa)
6330 Y=LGT(Ya/Ymin)*Sfy
6340 X=LGT(Xa/Xmin)*Sfx
6350 IF Y<0 THEN Y=0

```

```

5360 IF Y>100 THEN GOTO 5380
5370 PRINT "PA",X,Y,"PP"
5380 NEXT X
5390 END IC
5400 PRINT "PU PA 0.0 SP0"
5410 SUBEND
5420 DEF FNHsmooth(X,ItD)
5430 Hs=FNPoly(X)/X
5440 IF ItD=1 THEN Hs=Hs*.83347
5450 RETURN Hs
5460 FNEND
5470 DEF FNPoly(X)
5480 Poly=-4.4123718E+2-X*(6.8123917E+2-X*3.7416863E+2)
5490 RETURN Poly
5500 FNEND
5510 DEF FNPvst(Tsteam)
5515 DIM K(8)
5520 DATA -7.691234564,-26.08023696,-168.1706546,64.23285504,-118.9646225
5525 DATA 4.16711732,20.9750676,1.E9,6
5530 READ K(*)
5535 T=(Tsteam+273.15)/647.3
5540 Sum=0
5545 FOR N=0 TO 4
5550 Sum=Sum+K(N)*((1-T)^(N+1))
5555 NEXT N
5560 Br=Sum/(T*(1+K(5)*((1-T)+K(6)*((1-T)^2)))-((1-T)/(K(7)*((1-T)^2+K(8)))
5565 Pr=EXP(Br)
5570 P=22120000*Pr
5575 RETURN P
5580 FNEND

```

APPENDIX B

SAMPLE CALCULATIONS

Data set number fifteen of file GT6H29 corresponding to tube number 6 was chosen for the sample calculation.

A. TEST-SECTION DIMENSIONS

O.D.	=	25.30 (mm)
H_F	=	1.05 (mm)
fins/mm	=	1.02
inter-fin gap	=	0.25 (mm)
D_2	=	23.10 (mm)
D_1	=	17.86 (mm)
D_O	=	22.22 (mm)
D_i	=	20.32 (mm)
L_U	=	31.75 (mm)
L	=	50.80 (mm)

B. MEASURED PARAMETERS

V	=	70.0 (volts)
V_{RES}	=	4.8 (volts)
R	=	2.031 (ohms)
k_C	=	383 (W/m.K)
T_1	=	54.23 (°C)
T_2	=	54.29 (°C)
T_3	=	53.91 (°C)

$$\begin{aligned}
T_4 &= 53.65 \text{ (}^\circ\text{C)} \\
T_5 &= 53.40 \text{ (}^\circ\text{C)} \\
T_6 &= 53.31 \text{ (}^\circ\text{C)} \\
T_7 &= 53.22 \text{ (}^\circ\text{C)} \\
T_8 &= 53.54 \text{ (}^\circ\text{C)} \\
T_{\text{SAT}} &= 47.51 \text{ (}^\circ\text{C)}
\end{aligned}$$

C. PROPERTIES OF FREON-113 AT SATURATION TEMPERATURE

$$\begin{aligned}
\mu &= 4.948 \times 10^{-4} \text{ (kg/m.s)} \\
\rho &= 1510.0 \text{ (kg/m}^3\text{)} \\
C_p &= 0.973 \text{ (kJ/kg.K)} \\
k &= 0.0715 \text{ (W/m.K)}
\end{aligned}$$

D. HEAT-FLUX CALCULATION

The heat transfer rate from the cartridge heater:

$$Q_H = VI \text{ (W)} \quad \text{and} \quad I = V_{\text{RES}}/R \text{ (amps)}$$

$$I = 4.8/2.031 = 2.363 \text{ (amps)}$$

$$Q_H = 70.0 \times 2.363 = 165.410 \text{ (W)}$$

The cross-sectional area of machined ends:

$$A_C = \pi/4.0 (D_o^2 - D_i^2) \text{ (m}^2\text{)}$$

$$A_C = \pi/4.0 (0.02222^2 - 0.02032^2) = 63.481 \times 10^{-6} \text{ (m}^2\text{)}$$

The tube outside wall perimeter:

$$P = \pi D_o = 3.1416 \times 0.02222 = 6.981 \times 10^{-2} \text{ (m)}$$

The corrected length of ends:

$$L_C = L_U + t/2.0 \quad t = D_o - D_i$$

$$L_C = 0.03175 + (0.02222 - 0.02032)/2.0 = 32.7 \times 10^{-3} \text{ (m)}$$

Other thermophysical properties:

$$\nu = \mu/\rho = 4.948 \times 10^{-4}/1510.0 = 3.277 \times 10^{-7} \text{ (m}^2/\text{s)}$$

$$\alpha = k/\rho C_p = 0.0715/(1510.0 \times 973) = 4.866 \times 10^{-8} \text{ (m}^2/\text{s)}$$

$$\beta = -\frac{1}{\rho} \frac{\Delta \rho}{\Delta T} = -\frac{1}{1510} \left(\frac{1509.77 - 1510.26}{47.61 - 47.41} \right) \\ = 0.00162 \text{ (1/K)}$$

$$Pr = \nu/\alpha = 3.277 \times 10^{-7}/4.866 \times 10^{-8} = 6.734$$

Temperature at the base of the T-shaped fins:

$$T_B = T_{AVG} - Q_H \frac{\ln(D_2/D_1)}{2 \pi L k_C}$$

$$T_{AVG} = \left(\sum_{n=1}^8 T_N \right) / 8.0 = 53.69 \text{ (}^\circ\text{C)}$$

$$T_B = 53.69 - 165.41 \frac{\ln(23.1/17.86)}{2\pi \times 0.0508 \times 383} = 53.34 \text{ (}^\circ\text{C)}$$

$$\theta_B = T_B - T_{SAT} = 53.342 - 47.51 = 5.832 \text{ (K)}$$

Average heat-transfer coefficient at the unenhanced ends:

$$\bar{h} = \frac{k}{D_o} \left\{ 0.60 + 0.387 \frac{\left[\frac{g \beta D_o^3 \theta_B \text{Tanh}\left\{ \left(\frac{\bar{h} P}{k_{C A_C}} \right)^{1/2} L_C \right\}}{\nu \alpha L_C \left(\frac{\bar{h} P}{k_{C A_C}} \right)^{1/2}} \right]^{1/6}}{\left[1 + \left(0.559 / \text{Pr} \right)^{9/16} \right]^{8/27}} \right\}^2$$

$$\bar{h} = 187.49 \text{ (W/m}^2 \cdot \text{K)}$$

Heat-transfer rate through unenhanced ends:

$$Q_F = \sqrt{\bar{h} P k_{C A_C}} \theta_B \text{Tanh } mL_C$$

$$m = \left(\frac{\bar{h} P}{k_{C A_C}} \right)^{1/2} = \left(\frac{187.489 \times 6.981 \times 10^{-2}}{0.0715 \times 63.481 \times 10^{-6}} \right)^{1/2} = 1.698 \times 10^3$$

$$Q_F = 3.29 \text{ (W)}$$

$$Q_{LOSS} = 2Q_F = 6.579 \text{ (W)}$$

Heat flux through Gewa-T surface:

$$Q = Q_H - Q_{LOSS}$$

$$Q = 165.41 - 6.579 = 158.83 \text{ (W)}$$

$$q = Q/A_B$$

$$A_B = \pi \times 23.1 \times 10^{-3} \times 50.8 \times 10^{-3} = 3.687 \times 10^{-3} \text{ (m}^2\text{)}$$

$$q = \frac{158.83}{3.687 \times 10^{-3}} = 43.978 \times 10^3 \text{ (W/m}^2\text{)}$$

The following are the results obtained from the computer by running the data reduction program (DRP) (see Appendix A):

$$Q = 44.466 \text{ 10 (W/m}^2\text{)}$$

$$\theta_B = 5.76 \text{ (K)}$$

$$h = 187.39 \text{ (W/m}^2\text{.K)}$$

The small difference in results obey the inaccuracy of hand calculations with the use of about three significant digits only.

AD-A152 286

NUCLEATE POOL BOILING CHARACTERISTICS OF GEMA-T FINNED
SURFACES IN FREON-113(U) NAVAL POSTGRADUATE SCHOOL
MONTEREY CA R J PULIDO SEP 84

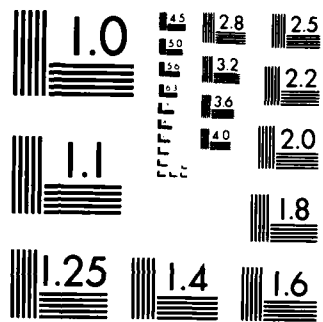
2/2

UNCLASSIFIED

F/G 20/13

NL





MICROCOPY RESOLUTION TEST CHART
NATIONAL BUREAU OF STANDARDS-1963-A

APPENDIX C

UNCERTAINTY ANALYSIS

The same data set (set No. 15 of file GT6H29) that was used for the sample calculation was chosen for the uncertainty analysis; therefore dimensions of test section, measured and calculated parameters found in sample calculation were used in this analysis. All uncertainties are presented as a percentage of the calculated parameter.

A. UNCERTAINTY IN SOURCE HEAT-TRANSFER RATE

$$Q = VI \text{ (W)}, \quad I = V_{\text{RES}}/R \text{ (amp)}$$

$$\delta V = \delta V_{\text{RES}} = 0.05 \text{ (volts)}$$

where:

δ = uncertainty in measurement and calculation

$$\delta I = \delta V_{\text{RES}}/R = 0.05/2.031 = 0.025 \text{ (amp)}$$

$$\frac{\delta Q_H}{Q_H} = \left[\left(\frac{\delta V}{V} \right)^2 + \left(\frac{\delta I}{I} \right)^2 \right]^{1/2}$$

$$\frac{\delta Q_H}{Q_H} = \left[\left(\frac{0.05}{70} \right)^2 + \left(\frac{0.025}{2.363} \right)^2 \right]^{1/2} = 1.06 \text{ percent}$$

B. UNCERTAINTY IN SURFACE AREA

$$A_B = \pi D_2 L \quad \delta D_2 = \delta L = 0.1 \text{ (mm)}$$

$$\frac{\delta A_B}{A_B} = \left[\left(\frac{0.1}{23.1} \right)^2 + \left(\frac{0.1}{50.8} \right)^2 \right]^{1/2} = 0.48 \text{ percent}$$

C. UNCERTAINTY IN ΔT

$$\Delta T = T_W - T_{SAT} \quad \delta T_W = \delta T_{SAT} = 0.15 \text{ (}^\circ\text{C)}$$

$$\frac{\delta \Delta T}{\Delta T} = \left[\left(\frac{\delta T_W}{\Delta T} \right)^2 + \left(- \frac{\delta T_{SAT}}{\Delta T} \right)^2 \right]^{1/2}$$

$$\frac{\delta \Delta T}{\Delta T} = \left[\left(\frac{0.15}{6.18} \right)^2 + \left(- \frac{0.15}{6.18} \right)^2 \right]^{1/2} = 3.43 \text{ percent}$$

D. UNCERTAINTY IN HEAT FLUX

$$q = \frac{Q_H - 2Q_F}{A_B}$$

$$\frac{\delta q}{q} = \left[\left(\frac{\delta Q_H}{Q_H - 2Q_F} \right)^2 + \left(\frac{2\delta Q_F}{Q_H - 2Q_F} \right)^2 + \left(- \frac{\delta A_B}{A_B} \right)^2 \right]^{1/2}$$

In this case, $Q_H = 165.41 \text{ (W)}$ and $Q_F = 3.29 \text{ (W)}$

Therefore, $Q_F = 2.0$ percent of Q_H . Assuming the same proportion in the uncertainty for Q_F :

$$\delta Q_F = 0.02 \delta Q_H = 0.02 \times 1.753 = 0.035 \text{ (W)}$$

$$\frac{\delta q}{q} = \left[\left(\frac{1.753}{158.83} \right)^2 + \left(-\frac{2 \times 0.035}{158.83} \right)^2 + (-0.0048)^2 \right]^{1/2}$$

$$\frac{\delta q}{q} = 1.26 \text{ percent}$$

E. UNCERTAINTY IN BOILING HEAT-TRANSFER COEFFICIENT

$$\bar{h} = \frac{q}{\Delta T}$$

$$\frac{\delta \bar{h}}{\bar{h}} = \left[\left(\frac{\delta q}{q} \right)^2 + \left(-\frac{\delta \Delta T}{\Delta T} \right)^2 \right]^{1/2}$$

$$\frac{\delta \bar{h}}{\bar{h}} = \left[(0.0126)^2 + (-0.0343)^2 \right]^{1/2} = 3.65 \text{ percent}$$

LIST OF REFERENCES

1. Marto, P., and Lepere, V., "Pool Boiling Heat Transfer from Enhanced Surfaces to Dielectric Fluids," Journal of Heat Transfer, vol. 104, May 1982, pp. 292-299.
2. Chongrungreon, S., and Sauer, Jr., H.T., "Nucleate Boiling Performance of Refrigerants and Refrigerant-Oil Mixtures," J. of Heat Transfer, vol. 102, pp. 701-705, 1980.
3. Van Stralew, S., and Cole, R., "Boiling Phenomena," v. 1, McGraw-Hill Book Company, 1979, p. 117.
4. Nishikawa, K., and Ito, T., "Augmentation of Nucleate Boiling Heat Transfer by Prepared Surfaces," Japan-United States Heat Transfer Joint Seminar, Tokyo, Sept. 1980.
5. Yilmaz, S., and Westwater, J., "Effect of Commercial Enhanced Surfaces on the Boiling Heat Transfer Curve," Advances in Enhanced Heat Transfer, p. 74, 1981.
6. Bergles, A., and Chyu, M., "Characteristics of Nucleate Pool Boiling from Porous Metallic Coatings," Advances in Enhanced Heat Transfer, pp. 63-64, 1981.
7. Marto, P., and Hernandez, B., "Nucleate Pool Boiling Characteristics of a Gewa-T Surface in Freon-113," Heat Transfer-Seattle 1983, No. 225, vol. 79, pp. 1-9.
8. Hernandez, B., "An Experimental Study of Nucleate Pool Boiling Heat Transfer from a Gewa-T Finned Surface in Freon-113," 1982, pp. 32-40.
9. Lepere, V., "Pool Boiling Heat Transfer from Enhanced Surfaces to Dielectric Fluids," 1981, pp. 37-41.
10. Incropera, F.P., and DeWitt, D.P., Fundamentals of Heat Transfer, John Wiley and Sons, Inc., New York, N.Y., p. 447, 1981.
11. Cornwell, K., Schuller, R., and Einarsson, J., "The Influence of Diameter on Nucleate Pool Boiling Outside Tubes," Heat Transfer, v. 4, pp. 47-52, 1982.
12. Rehm, J., and Bankoff, S., "Convective Boiling in a Narrow Concentric Annulus," AIAA 19th Thermophysics Conference, June 24-28, 1984, Snowmass, Colorado.

INITIAL DISTRIBUTION LIST

	No. Copies
1. Defense Technical Information Center Cameron Station Alexandria, Virginia 22314	2
2. Library, Code 0142 Naval Postgraduate School Monterey, California 93943	2
3. Department Chairman, Code 69 Department of Mechanical Engineering Naval Postgraduate School Monterey, California 93943	1
4. Professor Paul J. Marto, Code 69Mx Department of Mechanical Engineering Naval Postgraduate School Monterey, California 93943	2
5. Dr. A.S. Wanniarachchi, Code 69Wa Department of Mechanical Engineering Naval Postgraduate School Monterey, California 93943	1
6. Mr. Fred Weiler Wieland-America Incorporated Orange, New Jersey 07050	1
7. Mr. Klaus Menze Wieland Werke AG WEST GERMANY	1
8. TNEI Ricardo Pulido Apartado Aereo No. 5878 Cartagena COLOMBIA	1

END

FILMED

5-85

DTIC